cells and macrophages following stimulation with Toll-like receptor (TLR) ligands, induce expression of TGFβ3, leading to the induction of pathogenic Th17(23) cells (Lee et al., 2012). These pathogenic Th17 cells are characterized by the expression of T-bet (TBX21, T-box protein 21), a master regulator of Th1-cell development, as well as RORγt. Compared with Th1 and Th2 differentiation, Th17-cell differentiation exhibits plastic or flexible features (Oestreich and Weinmann, 2012; Basu et al., 2013). TGFβ1 signaling induces the expression of both Foxp3 and RORγt in antigen-activated naïve $CD4^+$ T cells and is involved in the differentiation of both iTreg and Th17 cells. Therefore, additional factors determine iTreg and Th17 polarization. Furthermore, iTreg and Th17 cells can transdifferentiate under specific conditions (Hoechst et al., 2011). The transition from Th17 cells to Th1 cells is also induced by IL23 and IL12 in a STAT4- and T-bet-dependent manner (Lee et al., 2009; Mukasa et al., 2010).

In addition to RORγt and the aforementioned cytokines, several transcriptional regulators positively regulate Th17 cell differentiation: signal transducer and activator of transcription 3 (STAT3), BATF (basic leucine zipper transcriptional factor, ATF-like), interferon regulatory factor 4 (IRF4), Runt-related transcriptional factor 1 (RUNX1), RORα and aryl hydrocarbon receptor (AHR, a nuclear receptor for a number of low-molecular weight chemicals such as the tryptophan photoproduct 6-formylindolo[3,2-b]carbazole (FICZ)) (Hirahara et al., 2010; Kurebayashi et al., 2013). Moreover, prostaglandin E2, ATP, and C-type lectin ligands act on antigen-presenting cells to facilitate Th17-cell differentiation. By contrast, IL4, interferon-γ (IFNγ), IL27, suppressor of cytokine signaling 3 (SOCS3), and STAT5 all suppress Th17-cell differentiation.

Tc17 cells

$CD8^+$ T cells develop into Tc17 cells in the presence of TGFβ1 and either IL6 or IL21, similar to the requirements for Th17-cell development (Intlekofer et al., 2008). Tc17 cells are also characterized by the expression of RORγt, STAT3, RORα and IL23R. However, Tc17 cells do not express Granzyme B, and they exhibit impaired cytotoxic activity relative to conventional cytotoxic $CD8^+$T cells (Huber et al., 2009). A recent report suggested that TGFβ signaling is not required for in vivo differentiation of Tc17 cells (Dwivedi et al., 2012).

γδ T cells

Two distinct subsets of $CD27^+$ or $CD27^-$ γδ T cells develop in the mouse fetal thymus: co-stimulation of TCR and CD27 induces $CD27^+$ γδ T cells to express T-bet and produce IFNγ whereas the absence of TCR signaling (or weak signaling) promotes the development of IL17A-producing $CD27^-$ γδ T cells, a process controlled by RORγt and RUNX1 (Cua and Tato, 2010; Prinz et al., 2013). Because peripheral $CD27^-$γδ T cells have permissive histone modification at loci involved in expression of not only Il17a but also Ifng, they can produce both IL17A and IFNγ upon stimulation with IL1β and IL23 (Schmolka et al., 2013). All innate IL17-producing lymphocytes, including γδ T cells, iNKT cells and LTi cells, express RORγt and develop in an IL6-independent manner (Cua and Tato, 2010).

iNKT cells

iNKT cells are activated in response to glycolipid antigens presented by CD1d (Cua and Tato, 2010; Guo et al., 2012). IL17A-producing iNKT cells develop in the thymus, and express RORγt and IL23R. A recent report suggested that iNKT cells can be induced to produce IL17A in the presence of TGFβ1 and IL1β (Monteiro et al., 2013).

LTi cells

Innate lymphoid cells (ILCs), a family of RAG1/2-negative lymphoid cells, require the common cytokine receptor γ-chain (also known as IL2RG) and inhibitor of DNA binding 2 (ID2), a transcriptional repressor (Guo et al., 2012; Fuchs and Colonna, 2013; Spits et al., 2013). LTi cells, which like NK cells are prototypical ILCs, belong to the Group 3 ILCs (ILC3s), defined by the production of IL17A and/or IL22 (Spits et al., 2013). ILC3s require the expression of RORγt for their development, express IL23R and IL1R, and produce IL17A and/or IL22 upon stimulation with IL23 or IL1β.

B cells

A recent report shows that Trypanosoma crusi promotes IL17A production by B cells in human and mouse (Bermejo et al., 2013). T. crusi trans-sialidase mediates addition of sialyl residues onto CD45 expressed on B cells, resulting in induction of IL17A and F via BTK activation without the involvement of the transcriptional factors RORγt and AHR.

Other cells

Although the details of the underlying signaling pathways and transcriptional factors are not known, cells other than lymphocytes, such as Paneth cells in the gut and $CD11b^+Gr1^+$ cells in the injured kidney also produce IL17A (Cua and Tato, 2010).

Localisation

IL17A is a secreted protein.

Function

IL17A is a pro-inflammatory cytokine that acts on a variety of cells (e.g., fibroblasts, epithelial cells, endothelial cells, and monocytes) to induce the production of other cytokines, including IL6, tumor necrosis factor-α (TNFα), granulocyte-macrophage colony-stimulating-factor (GMCSF), granulocyte

colony-stimulating-factor (GCSF), chemokines (chemokine (C-X-C motif) ligand 1 (CXCL1), CXCL2, CXCL5, and CXCL8), antimicrobial peptides (defensins) and matrix metalloproteinases (MMP1, MMP3, and MMP13) (Eyerich et al., 2010; Iwakura et al., 2011). These factors mediate the recruitment, activation and migration of neutrophils and myeloid cells, and also induce angiogenesis and tissue destruction.

IL17A, IL17F, and the IL17A-IL17F heterodimer bind to a heteromeric receptor complex composed of IL17 receptor A (IL17RA) and IL17 receptor C (IL17RC). IL17RA is expressed at high levels in hematopoietic cells and at low levels in epithelial cells, fibroblasts, and endothelial cells (Gaffen, 2009; Iwakura et al., 2011). On the other hand, IL17RC is expressed at low levels in hematopoietic cells and at high levels in the adrenal gland, prostate, liver, and thyroid. IL17RA has higher affinity for IL17A than IL17F, whereas IL17RC has higher affinity for IL17F than IL17A. Although cytokines secreted by most activated helper T cells generally stimulate the Janus kinase (JAK)/STAT pathway, the IL17-family cytokines stimulate signaling pathways involved in the innate immune system, such as the TLR signaling pathway (Gaffen, 2009; Iwakura et al., 2011).

IL17 receptors contain a conserved domain, 'similar expression to fibroblast growth factor/IL17R' (SEFIR), in the cytoplasmic region. This domain is similar to the Toll-/IL1R (TIR) domain (Gaffen, 2009; Iwakura et al., 2011). When the IL17 receptor is activated, the adaptor molecule actin-related gene 1 (ACT1, a U-box E3 ubiquitin ligase) is recruited to the SEFIR domain and mediates the lysine 63-linked ubiquitination of tumor necrosis factor receptor-associated factor 6 (TRAF6) (Gaffen, 2009; Iwakura et al., 2011). Ubiquitinated TRAF6 then activates the transcriptional factor nuclear factor κB (NFκB), various mitogen-activated protein (MAP) kinases including ERKs and p38, and CCAAT/enhancer-binding proteins (C/EBPβ and C/EBPδ).

IL-17A expression and Th17 cell development are remarkably affected not only by microorganisms and tumors, but also by several environmental factors such as nutrients, metabolites, hypoxia, toxins, NaCl concentrations, and circadian rhythm.

The tryptophan photoproduct FICZ positively regulates Th17-cell differentiation through AHR, whereas 2,3,7,8-tetrachlorodibezo-p-dioxin (TCDD) negatively regulates differentiation through that receptor (Quintana et al., 2008; Veldhoen et al., 2008). Activation of mTORC1 (mTOR complex containing mLST8 and Raptor) promotes Th17-cell differentiation via positive regulation of hypoxia-inducible factor 1α (HIF1α expression and the activation of S6 kinase (Barbi et al., 2013; Kurebayashi et al., 2013). HIF1α directly upregulates expression of RORγt and IL17A. Therefore, amino acid deprivation selectively blocks Th17-cell development through inhibition of mTORC1, whereas hypoxia promotes Th17 development through the activation of HIF1α. High levels of lactic acid, secreted from tumors due to the Warburg effect, induce macrophages or monocytes to mediate increased IL17A production by Th17 cells in an antigen-dependent manner, but do not Th17-cell differentiation or proliferation (Shime et al., 2008; Yabu et al., 2011).

The circadian rhythm is controlled by a series of feedback loops between the transcriptional factors, a CLOCK-BMAL1 complex and REV-ERBα (Arjona et al., 2012). The expression of RORγt is suppressed by the leucine zipper transcriptional factor NFIL3, which is negatively regulated by REV-ERBα (Yu et al., 2013). Accordingly, $CD4^+$ T cells purified during the day express RORγt at higher levels than those purified at night, and tend to differentiate into Th17 cells.

High salt concentration (e.g., 40 mM NaCl) induces phosphorylation of p38 and the expression of serum glucocorticoid kinase 1 (SGK1) and nuclear factor of activated T-cells 5 (NFAT5) to promote the IL23-dependent differentiation of pathogenic Th17 cells (Kleinewietfeld et al., 2013; Wu et al., 2013a). In vivo, a high salt diet promotes Th17-cell differentiation and exacerbates neuropathy in mice with experimental autoimmune encephalomyelitis.

Homology

IL17A is a prototypical member of the IL17 family. This family includes six proteins: IL17A, IL17B, IL17C, IL17D, IL17E (also called IL25), and IL17F. Interleukins 17A-F are not homologous to any other known proteins. IL17A has the highest sequence identity with IL17F (46.5 %). It is less similar to the other IL17 family members: IL17B, 26.4 %; IL17C, 28.9 %; IL17D, 21.8 %; and IL17E, 17.7 %.

Implicated in

Ovarian cancer

Note

Tumor infiltration by Th17 cells is positively correlated with infiltration by Th1 cells, IFNγ-producing $CD8^+$ cells (Tc1 cells), IL17A- and IFNγ-double-positive T cells, and NK cells, but negatively correlated with the presence of Treg cells (Kryczek et al., 2009a). Increased IL17A levels in ascites are well correlated with better patient survival and lower grades of ovarian cancer.

Esophageal cancer

Note

Elevated levels of IL17A-producing cells, including Th17 cells, in esophageal cancer tissues are

associated with the intratumoral accumulation of $CD8^+$ T and NK cells, as well as with better prognosis (Lv et al., 2011).

Prostate cancer

Note

In prostate tumors, elevated levels of Th17 cells are associated with a lower pathologic Gleason scores (Sfanos et al., 2008). However, in prostate cancer patients, a higher frequency of $CCR4^-$ Th17 cells in peripheral blood is correlated with shorter time to metastatic progression after immunotherapy with an allogeneic whole-cell vaccine (Derhovanessian et al., 2009).

Gastric cancer

Note

The relationship between IL17A and gastric cancer is controversial. Expression of IL17A in peripheral blood mononuclear cells (PBMC) and gastric cancer tissue is elevated, especially in patients with advanced-stage gastric cancer (Zhang et al., 2008; Zhuang et al., 2012; Su et al., 2014). One group suggested that increased infiltration of Tc17 cells in tissues is associated with higher stages and lower overall survival rates (Zhuang et al., 2012). Th17 cells also infiltrate tumors, but the percentage of Th17 cells is lower than that of Tc17 cells. CXCL12, which is produced by tumors stimulated with IL17A, promotes the recruitment of CXCR4-dependent MDSCs and suppresses the function of the cytotoxic $CD8^+$ T cells (Zhuang et al., 2012). However, another group's report showed that intratumoral expression of IL17A is associated with good prognosis (Chen et al., 2011). Several studies have examined the relationship between gastric cancer risk and a single nucleotide polymorphism (SNP) in the IL17A gene promoter region. This SNP (rs2275913, G/A SNP, 52051033 bp from pter) is located at position -197 relative to the start codon within the NFAT-binding motif. The A-allele is associated with higher IL17A promoter activity and higher affinity for NFAT, which plays critical roles in the IL17A production, than the G-allele (Espinoza et al., 2011). Studies of the association between rs2275913 and gastric cancer have yielded different results in different populations. Four groups reported that the AA-genotype and A-allele of SNP rs2275913 are significantly associated with gastric cancer risk in Japanese (Shibata et al., 2009), Iranian (Rafiei et al., 2013), and Chinese populations (Qinghai et al., 2014; Zhang et al., 2014a), whereas one Chinese group reported that this SNP is not associated with total cancer risk or survival in gastric cancer patients (Wu et al., 2010). Two studies suggested that this SNP is significantly associated with gastric cancer risk in Helicobacter pylori-infected patients, smokers, or non-cardia gastric cancer patients (Qinghai et al., 2014; Zhang et al., 2014a). The TT-genotype of the SNP rs3748067, which is localized in 3' UTR of the IL17A gene (C/T SNP, a position at 52055339 bp from pter), was associated with increased risk of gastric cancer in two studies (Qinghai et al., 2014; Zhang et al., 2014a).

Colorectal cancer

Note

Elevated levels of IL17A-producing cells are associated with poor prognosis as a result of increased VEGFA expression in colorectal cancer patients (Liu et al., 2011; Tosolini et al., 2011; Wu et al., 2013b). Furthermore, the A-allele of SNP rs2275913 is positively associated with susceptibility to colorectal cancer, as well as with clinical features as tumor location, tumor differentiation, and TNM stage (Omrane et al., 2014). In a mouse model of colorectal cancer, loss of effective barrier function in the transformed epithelial cells of colonic adenoma results in the infiltration of non-pathogenic bacteria and their products, leading to the production of inflammatory cytokines (including IL23 and IL17A) and the induction of tumor-elicited inflammation, which promotes tumor development (Grivennikov et al., 2012).

Hepatocellular cancer

Note

In patients with hepatocellular carcinoma, increased intratumoral accumulation of IL17A-producing cells is significantly associated with poor prognosis and increased tumor vasculogenesis (Zhang et al., 2009).

Uterine cervical cancer

Note

Levels of Tc17 cells are higher in PBMCs and tumors of uterine cervical cancer patients with lymph-node metastasis than in patients without metastasis (Zhang et al., 2014b). Higher accumulation of Tc17 cells in tumors is associated with a greater degree of tumor vasculogenesis and increased infiltration by Th17 cells and Treg cells. In Chinese women, the AA-genotype and A-allele of IL17A polymorphism rs2275913 are positively associated with susceptibility, peritumoral intravascular cancer emboli, and high clinical stage (Quan et al., 2012).

Breast cancer

Note

Increased infiltration of IL17A-producing cells in tissues is associated with shorter disease-free survival in breast cancer patients and higher histopathological grades (Chen et al., 2013). Among Han Chinese women, the frequency of the AA-genotype of the IL17A SNP rs2275913 is also

higher in patients than controls (Wang et al., 2012). IL17A-producing T cells and Treg cells are synchronically increased in peripheral blood and tumor tissues of breast cancer patients relative to those of healthy individuals (Benevides et al., 2013). Levels of the angiogenic factors CXCL8, MMP-2, MMP-9, and VEGFA, which are induced by IL17A, are also elevated in breast cancer tissue. Thus, IL17A is an important prognostic factor in breast cancer.

Lung cancer

Note

Higher levels of IL17A-producing cells are associated with poor prognosis and increased lymphangiogenesis in non-small cell lung cancer tissues (Chen et al., 2010). Although no significant relationship between SNP rs2275913 in the IL17A gene and lung cancer risk has been observed in the total Tunisian population, the A-allele is associated with increased lung cancer risk in the male and smoker subgroups (Kaabachi et al., 2014).

Bladder cancer

Note

The frequency of the AA-genotype and A-allele of SNP rs2275913 in bladder cancer patients is significantly higher than in control Han Chinese populations (Zhou et al., 2013). This SNP is also associated with increased bladder cancer risk in males and non-smokers, as well as with invasion of bladder cancer.

Autoimmune and inflammatory diseases

Note

IL17-producing cells are associated with the pathogenesis of many autoimmune and inflammatory diseases, such as EAE/multiple sclerosis, inflammatory skin diseases/psoriasis, inflammatory bowel diseases, ankylosing spondylitis, and experimental arthritis/rheumatoid arthritis, in both human patients and mouse models (Awasthi and Kuchroo, 2009; Korn et al., 2009). Recent reports have shown that treatment of psoriasis patients with the antibodies that neutralize IL17A and IL17A-IL17F heterodimer or block IL17RA results in reduction in the affected skin area and disease severity (Leonardi et al., 2012; Papp et al., 2012). Thus, therapies targeting the IL17A signaling pathway are predicted to be effective in psoriasis patients.

Infections

Note

Both IL17A and IL17F are preferentially produced during infections with the Gram-negative bacteria Klebsiella pneumoniae in the lungs and Citrobacter rodentium in the colon, the Gram-positive bacterium Staphylococcus aureus in the skin, and the fungus Candida albicans in the mouth; IL17A appears to protect against all of these types of infections (Korn et al., 2009; O'Connor et al., 2010; Iwakura et al., 2011). During the early response to infection, IL17A is predominantly secreted by γδ T cells and iNKT cells, and it induces the production of antimicrobial peptides such as β-defensins, regenerating (REG) proteins, and S100 proteins, as well as granulopoietic factors such as GCSF and CCL20, from epithelial cells (Cua and Tato, 2010). This results in the rapid recruitment of neutrophils to sites of infection, which in turn promotes efficient pathogen clearance. Later, antigen-specific αβ Th17 cells contribute to further responses to infection.

Cancers in mouse models

Note

Elevated expression of IL17A and increased accumulation of IL17A-producing cells in the tumor microenvironment are associated with anti-tumor or pro-tumor effects in various types of cancer in human patients and mouse models (Zou and Restifo, 2010). Although IL17A-producing cells are not the dominant T-cell subset in the tumor microenvironment, their levels are elevated to a greater extent in the tumor site than in peripheral blood of patients (Kryczek et al., 2009a). Recent reports have suggested that the increased accumulation of not only Th17 cells, but also Tc17 (Hinrichs et al., 2009; Zhuang et al., 2012), IL17-producing γδ T cells (Wakita et al., 2010; Schmolka et al., 2013), and ILC3s (Kirchberger et al., 2013), regulates tumor development.

Overexpression of IL17A in tumor cells suppresses tumor growth in a cytotoxic T lymphocyte-dependent manner (Benchetrit et al., 2002). The transfer of tumor antigen-specific T cells polarized to the IL17-producing phenotype also induces eradication of tumor cells by inducing strong $CD8^+$ T-cell activation (Martin-Orozco et al., 2009). Furthermore, deficiency of IL17A in mice promotes growth and metastasis of tumors (Kryczek et al., 2009b; Martin-Orozco et al., 2009). IL17A-producing T cells are predicted to induce recruitment of other effector cells (e.g., cytotoxic $CD8^+$ T cells and NK cells) to tumors by inducing expression of CXCL9 and CXCL10 within tumor sites (Kryczek et al., 2009a). Moreover, Th17 cells induce expression of CCL20, a ligand for chemokine (C-C motif) receptor 6 (CCR6), in tumor tissues. CCL20 recruits dendritic cells, which mediate anti-tumor effects in a CCL20/CCR6-dependent manner (Martin-Orozco et al., 2009).

On the other hand, overexpression of IL17A in tumors facilitates tumor growth by inducing angiogenesis in the tumor microenvironment (Numasaki et al., 2003; Numasaki et al., 2005).

Furthermore, IL17A-deficient or IL17RA-deficient mouse models were used to show that IL17A was involved in the promotion of tumor growth via induction of myeloid-derived suppressor cells (MDSC) (He et al., 2010), activation of IL6-STAT3 pathway (Wang et al., 2009), and elevated angiogenesis (Wakita et al., 2010). The discrepancies between anti-tumor and pro-tumor effects may be due to the distinct roles of IL17A-producing cells in different tumors.

A recent report showed that IL17A is involved in tumor resistance to anti-angiogenic therapy targeting vascular endothelial growth factor A (VEGFA) (Chung et al., 2013). In this case, the primary effect of IL17A is the induction of granulocyte colony-stimulating factor (GCSF) expression in tumor-associated fibroblasts, leading to recruitment of MDSC in the tumor microenvironment and induction of another angiogenic factor, prokineticin 2 (PROK2, Bv8). These results suggest that inhibition of IL17A function may improve the efficacy of anti-angiogenic therapies.

References

McDonald NQ, Hendrickson WA. A structural superfamily of growth factors containing a cystine knot motif. Cell. 1993 May 7;73(3):421-4

Rouvier E, Luciani MF, Mattéi MG, Denizot F, Golstein P. CTLA-8, cloned from an activated T cell, bearing AU-rich messenger RNA instability sequences, and homologous to a herpesvirus saimiri gene. J Immunol. 1993 Jun 15;150(12):5445-56

Hymowitz SG, Filvaroff EH, Yin JP, Lee J, Cai L, Risser P, Maruoka M, Mao W, Foster J, Kelley RF, Pan G, Gurney AL, de Vos AM, Starovasnik MA. IL-17s adopt a cystine knot fold: structure and activity of a novel cytokine, IL-17F, and implications for receptor binding. EMBO J. 2001 Oct 1;20(19):5332-41

Benchetrit F, Ciree A, Vives V, Warnier G, Gey A, Sautès-Fridman C, Fossiez F, Haicheur N, Fridman WH, Tartour E. Interleukin-17 inhibits tumor cell growth by means of a T-cell-dependent mechanism. Blood. 2002 Mar 15;99(6):2114-21

Numasaki M, Fukushi J, Ono M, Narula SK, Zavodny PJ, Kudo T, Robbins PD, Tahara H, Lotze MT. Interleukin-17 promotes angiogenesis and tumor growth. Blood. 2003 Apr 1;101(7):2620-7

Kolls JK, Lindén A. Interleukin-17 family members and inflammation. Immunity. 2004 Oct;21(4):467-76

Numasaki M, Watanabe M, Suzuki T, Takahashi H, Nakamura A, McAllister F, Hishinuma T, Goto J, Lotze MT, Kolls JK, Sasaki H. IL-17 enhances the net angiogenic activity and in vivo growth of human non-small cell lung cancer in SCID mice through promoting CXCR-2-dependent angiogenesis. J Immunol. 2005 Nov 1;175(9):6177-89

Intlekofer AM, Banerjee A, Takemoto N, Gordon SM, Dejong CS, Shin H, Hunter CA, Wherry EJ, Lindsten T, Reiner SL. Anomalous type 17 response to viral infection by CD8+ T cells lacking T-bet and eomesodermin. Science. 2008 Jul 18;321(5887):408-11

Quintana FJ, Basso AS, Iglesias AH, Korn T, Farez MF, Bettelli E, Caccamo M, Oukka M, Weiner HL. Control of T(reg) and T(H)17 cell differentiation by the aryl hydrocarbon receptor. Nature. 2008 May 1;453(7191):65-71

Sfanos KS, Bruno TC, Maris CH, Xu L, Thoburn CJ, DeMarzo AM, Meeker AK, Isaacs WB, Drake CG. Phenotypic analysis of prostate-infiltrating lymphocytes reveals TH17 and Treg skewing. Clin Cancer Res. 2008 Jun 1;14(11):3254-61

Shime H, Yabu M, Akazawa T, Kodama K, Matsumoto M, Seya T, Inoue N. Tumor-secreted lactic acid promotes IL-23/IL-17 proinflammatory pathway. J Immunol. 2008 Jun 1;180(11):7175-83

Veldhoen M, Hirota K, Westendorf AM, Buer J, Dumoutier L, Renauld JC, Stockinger B. The aryl hydrocarbon receptor links TH17-cell-mediated autoimmunity to environmental toxins. Nature. 2008 May 1;453(7191):106-9

Zhang B, Rong G, Wei H, Zhang M, Bi J, Ma L, Xue X, Wei G, Liu X, Fang G. The prevalence of Th17 cells in patients with gastric cancer. Biochem Biophys Res Commun. 2008 Sep 26;374(3):533-7

Awasthi A, Kuchroo VK. Th17 cells: from precursors to players in inflammation and infection. Int Immunol. 2009 May;21(5):489-98

Derhovanessian E, Adams V, Hähnel K, Groeger A, Pandha H, Ward S, Pawelec G. Pretreatment frequency of circulating IL-17+ CD4+ T-cells, but not Tregs, correlates with clinical response to whole-cell vaccination in prostate cancer patients. Int J Cancer. 2009 Sep 15;125(6):1372-9

Ely LK, Fischer S, Garcia KC. Structural basis of receptor sharing by interleukin 17 cytokines. Nat Immunol. 2009 Dec;10(12):1245-51

Gaffen SL. Structure and signalling in the IL-17 receptor family. Nat Rev Immunol. 2009 Aug;9(8):556-67

Gerhardt S, Abbott WM, Hargreaves D, Pauptit RA, Davies RA, Needham MR, Langham C, Barker W, Aziz A, Snow MJ, Dawson S, Welsh F, Wilkinson T, Vaugan T, Beste G, Bishop S, Popovic B, Rees G, Sleeman M, Tuske SJ, Coales SJ, Hamuro Y, Russell C. Structure of IL-17A in complex with a potent, fully human neutralizing antibody. J Mol Biol. 2009 Dec 18;394(5):905-21

Hinrichs CS, Kaiser A, Paulos CM, Cassard L, Sanchez-Perez L, Heemskerk B, Wrzesinski C, Borman ZA, Muranski P, Restifo NP. Type 17 CD8+ T cells display enhanced antitumor immunity. Blood. 2009 Jul 16;114(3):596-9

Huber M, Heink S, Grothe H, Guralnik A, Reinhard K, Elflein K, Hünig T, Mittrücker HW, Brüstle A, Kamradt T, Lohoff M. A Th17-like developmental process leads to CD8(+) Tc17 cells with reduced cytotoxic activity. Eur J Immunol. 2009 Jul;39(7):1716-25

Korn T, Bettelli E, Oukka M, Kuchroo VK. IL-17 and Th17 Cells. Annu Rev Immunol. 2009;27:485-517

Kryczek I, Banerjee M, Cheng P, Vatan L, Szeliga W, Wei S, Huang E, Finlayson E, Simeone D, Welling TH, Chang A, Coukos G, Liu R, Zou W. Phenotype, distribution, generation, and functional and clinical relevance of Th17 cells in the human tumor environments. Blood. 2009a Aug 6;114(6):1141-9

Kryczek I, Wei S, Szeliga W, Vatan L, Zou W. Endogenous IL-17 contributes to reduced tumor growth and metastasis. Blood. 2009b Jul 9;114(2):357-9

Lee YK, Turner H, Maynard CL, Oliver JR, Chen D, Elson CO, Weaver CT. Late developmental plasticity in the T helper 17 lineage. Immunity. 2009 Jan 16;30(1):92-107

Martin-Orozco N, Muranski P, Chung Y, Yang XO, Yamazaki T, Lu S, Hwu P, Restifo NP, Overwijk WW, Dong C. T helper 17 cells promote cytotoxic T cell activation in tumor immunity. Immunity. 2009 Nov 20;31(5):787-98

Shibata T, Tahara T, Hirata I, Arisawa T. Genetic polymorphism of interleukin-17A and -17F genes in gastric carcinogenesis. Hum Immunol. 2009 Jul;70(7):547-51

Wang L, Yi T, Kortylewski M, Pardoll DM, Zeng D, Yu H. IL-17 can promote tumor growth through an IL-6-Stat3 signaling pathway. J Exp Med. 2009 Jul 6;206(7):1457-64

Zhang JP, Yan J, Xu J, Pang XH, Chen MS, Li L, Wu C, Li SP, Zheng L. Increased intratumoral IL-17-producing cells correlate with poor survival in hepatocellular carcinoma patients. J Hepatol. 2009 May;50(5):980-9

Chen X, Wan J, Liu J, Xie W, Diao X, Xu J, Zhu B, Chen Z. Increased IL-17-producing cells correlate with poor survival and lymphangiogenesis in NSCLC patients. Lung Cancer. 2010 Sep;69(3):348-54

Cua DJ, Tato CM. Innate IL-17-producing cells: the sentinels of the immune system. Nat Rev Immunol. 2010 Jul;10(7):479-89

Eyerich S, Eyerich K, Cavani A, Schmidt-Weber C. IL-17 and IL-22: siblings, not twins. Trends Immunol. 2010 Sep;31(9):354-61

Ghoreschi K, Laurence A, Yang XP, Tato CM, McGeachy MJ, Konkel JE, Ramos HL, Wei L, Davidson TS, Bouladoux N, Grainger JR, Chen Q, Kanno Y, Watford WT, Sun HW, Eberl G, Shevach EM, Belkaid Y, Cua DJ, Chen W, O'Shea JJ. Generation of pathogenic T(H)17 cells in the absence of TGF-β signalling. Nature. 2010 Oct 21;467(7318):967-71

He D, Li H, Yusuf N, Elmets CA, Li J, Mountz JD, Xu H. IL-17 promotes tumor development through the induction of tumor promoting microenvironments at tumor sites and myeloid-derived suppressor cells. J Immunol. 2010 Mar 1;184(5):2281-8

Hirahara K, Ghoreschi K, Laurence A, Yang XP, Kanno Y, O'Shea JJ. Signal transduction pathways and transcriptional regulation in Th17 cell differentiation. Cytokine Growth Factor Rev. 2010 Dec;21(6):425-34

Mukasa R, Balasubramani A, Lee YK, Whitley SK, Weaver BT, Shibata Y, Crawford GE, Hatton RD, Weaver CT. Epigenetic instability of cytokine and transcription factor gene loci underlies plasticity of the T helper 17 cell lineage. Immunity. 2010 May 28;32(5):616-27

O'Connor W Jr, Zenewicz LA, Flavell RA. The dual nature of T(H)17 cells: shifting the focus to function. Nat Immunol. 2010 Jun;11(6):471-6

Wakita D, Sumida K, Iwakura Y, Nishikawa H, Ohkuri T, Chamoto K, Kitamura H, Nishimura T. Tumor-infiltrating IL-17-producing gammadelta T cells support the progression of tumor by promoting angiogenesis. Eur J Immunol. 2010 Jul;40(7):1927-37

Wu X, Zeng Z, Chen B, Yu J, Xue L, Hao Y, Chen M, Sung JJ, Hu P. Association between polymorphisms in interleukin-17A and interleukin-17F genes and risks of gastric cancer. Int J Cancer. 2010 Jul 1;127(1):86-92

Zou W, Restifo NP. T(H)17 cells in tumour immunity and immunotherapy. Nat Rev Immunol. 2010 Apr;10(4):248-56

Chen JG, Xia JC, Liang XT, Pan K, Wang W, Lv L, Zhao JJ, Wang QJ, Li YQ, Chen SP, He J, Huang LX, Ke ML, Chen YB, Ma HQ, Zeng ZW, Zhou ZW, Chang AE, Li Q. Intratumoral expression of IL-17 and its prognostic role in gastric adenocarcinoma patients. Int J Biol Sci. 2011 Jan 11;7(1):53-60

Espinoza JL, Takami A, Nakata K, Onizuka M, Kawase T, Akiyama H, Miyamura K, Morishima Y, Fukuda T, Kodera Y, Nakao S. A genetic variant in the IL-17 promoter is functionally associated with acute graft-versus-host disease after unrelated bone marrow transplantation. PLoS One. 2011;6(10):e26229

Hoechst B, Gamrekelashvili J, Manns MP, Greten TF, Korangy F. Plasticity of human Th17 cells and iTregs is orchestrated by different subsets of myeloid cells. Blood. 2011 Jun 16;117(24):6532-41

Iwakura Y, Ishigame H, Saijo S, Nakae S. Functional specialization of interleukin-17 family members. Immunity. 2011 Feb 25;34(2):149-62

Liu J, Duan Y, Cheng X, Chen X, Xie W, Long H, Lin Z, Zhu B. IL-17 is associated with poor prognosis and promotes angiogenesis via stimulating VEGF production of cancer cells in colorectal carcinoma. Biochem Biophys Res Commun. 2011 Apr 8;407(2):348-54

Lv L, Pan K, Li XD, She KL, Zhao JJ, Wang W, Chen JG, Chen YB, Yun JP, Xia JC. The accumulation and prognosis value of tumor infiltrating IL-17 producing cells in esophageal squamous cell carcinoma. PLoS One. 2011 Mar 31;6(3):e18219

Tosolini M, Kirilovsky A, Mlecnik B, Fredriksen T, Mauger S, Bindea G, Berger A, Bruneval P, Fridman WH, Pagès F, Galon J. Clinical impact of different classes of infiltrating T cytotoxic and helper cells (Th1, th2, treg, th17) in patients with colorectal cancer. Cancer Res. 2011 Feb 15;71(4):1263-71

Yabu M, Shime H, Hara H, Saito T, Matsumoto M, Seya T, Akazawa T, Inoue N. IL-23-dependent and -independent enhancement pathways of IL-17A production by lactic acid. Int Immunol. 2011 Jan;23(1):29-41

Arjona A, Silver AC, Walker WE, Fikrig E. Immunity's fourth dimension: approaching the circadian-immune connection. Trends Immunol. 2012 Dec;33(12):607-12

Dwivedi VP, Tousif S, Bhattacharya D, Prasad DV, Van Kaer L, Das J, Das G. Transforming growth factor-β protein inversely regulates in vivo differentiation of interleukin-17 (IL-17)-producing CD4+ and CD8+ T cells. J Biol Chem. 2012 Jan 27;287(5):2943-7

Grivennikov SI, Wang K, Mucida D, Stewart CA, Schnabl B, Jauch D, Taniguchi K, Yu GY, Osterreicher CH, Hung KE, Datz C, Feng Y, Fearon ER, Oukka M, Tessarollo L, Coppola V, Yarovinsky F, Cheroutre H, Eckmann L, Trinchieri G, Karin M. Adenoma-linked barrier defects and microbial products drive IL-23/IL-17-mediated tumour growth. Nature. 2012 Nov 8;491(7423):254-8

Guo L, Junttila IS, Paul WE. Cytokine-induced cytokine production by conventional and innate lymphoid cells. Trends Immunol. 2012 Dec;33(12):598-606

Lee Y, Awasthi A, Yosef N, Quintana FJ, Xiao S, Peters A, Wu C, Kleinewietfeld M, Kunder S, Hafler DA, Sobel RA, Regev A, Kuchroo VK. Induction and molecular signature of pathogenic TH17 cells. Nat Immunol. 2012 Oct;13(10):991-9

Leonardi C, Matheson R, Zachariae C, Cameron G, Li L, Edson-Heredia E, Braun D, Banerjee S. Anti-interleukin-17

uicc global cancer control

IJC
International Journal of Cancer

Development of a dendritic cell-targeting lipopeptide as an immunoadjuvant that inhibits tumor growth without inducing local inflammation

Takashi Akazawa[1], Toshimitsu Ohashi[1,2], Hiroko Nakajima[3], Yasuko Nishizawa[4], Ken Kodama[5], Kikuya Sugiura[6], Toshio Inaba[6] and Norimitsu Inoue[1]

[1] Department of Molecular Genetics, Osaka Medical Center for Cancer and Cardiovascular Diseases, Higashinari-ku, Osaka, Japan
[2] Department of Otolaryngology, Gifu University Graduate School of Medicine, Gifu, Japan
[3] Department of Cancer Immunology, Osaka University Graduate School of Medicine, Suita, Osaka, Japan
[4] Department of Pathology, Osaka Medical Center for Cancer and Cardiovascular Diseases Higashinari-ku, Osaka, Japan
[5] Department of Thoracic Surgery, Yao Municipal Hospital, Yao, Osaka, Japan
[6] Department of Advanced Pathobiology, Graduate School of Life and Environmental Sciences, Osaka Prefecture University, Izumisano, Osaka, Japan

Materials used for the past 30 years as immunoadjuvants induce suboptimal antitumor immune responses and often cause undesirable local inflammation. Some bacterial lipopeptides that act as Toll-like receptor (TLR) 2 ligands activate immune cells as immunoadjuvants and induce antitumor effects. Here, we developed a new dendritic cell (DC)-targeting lipopeptide, h11c (P2C-ATPEDNGRSFS), which uses the CD11c-binding sequence of intracellular adhesion molecule-1 to selectively and efficiently activate DCs but not other immune cells. Although the h11c lipopeptide activated DCs similarly to an artificial lipopeptide, P2C-SKKKK (P2CSK4), *via* TLR2 *in vitro*, h11c induced more effective tumor inhibition than P2CSK4 at low doses *in vivo* with tumor antigens. Even without tumor antigens, h11c lipopeptide significantly inhibited tumor growth and induced tumor-specific cytotoxic T cells. P2CSK4 was retained subcutaneously at the vaccination site and induced severe local inflammation in *in vivo* experiments. In contrast, h11c was not retained at the vaccination site and was transported into the tumor within 24 hr. The recruitment of DCs into the tumor was induced by h11c more effectively, while P2CSK4 induced the accumulation of neutrophils leading to severe inflammation at the vaccination site. Because CD11b+ cells, but not CD11c+ cells, produced neutrophil chemotactic factors such as macrophage inflammatory protein (MIP)-2 in response to stimulation with TLR2 ligands, the DC-targeting lipopeptide h11c induced less MIP-2 production by splenocytes than P2CSK4. In this study, we succeeded in developing a novel immunoadjuvant, h11c, which effectively induces antitumor activity without adverse effects such as local inflammation *via* the selective activation of DCs.

Key words: immunoadjuvant, cancer immunotherapy, toll-like receptor, lipopeptide

Abbreviations: BCG: *Mycobacterium bovis* bacillus Calmette-Guérin; BMDCs: bone marrow-derived dendritic cells; CTL: cytotoxic T lymphocyte; CWS: cell-wall skeleton; DCs: dendritic cells; FACS: fluorescence-activated cell sorter; FITC: fluorescein isothiocyanate; GM-CSF: granulocyte-macrophage colony-stimulating factor; ICAM-1: intracellular adhesion molecule-1; MALP-2: macrophage-activating lipopeptide-2; MIP-2: macrophage inflammatory protein-2; TLR: toll-like receptor; WT1: Wilms tumor 1

Additional Supporting Information may be found in the online version of this article.

Grant sponsor: Japan Society for the Promotion of Science and the Ministry of Education, Culture, Science, and Technology; **Grant numbers:** 24590500, 21790400, 20200075

DOI: 10.1002/ijc.28939

History: Received 27 Dec 2013; Accepted 15 Apr 2014; Online 00 Month 2014

Correspondence to: Takashi Akazawa, Department of Molecular Genetics, Osaka Medical Center for Cancer and Cardiovascular Diseases, 1-3-2 Nakamichi, Higashinari-ku, Osaka 537-8511, Japan, Tel: +81-6-69-72-85-11, Fax: +81-6-69-73-56-91, E-mail: akazawa-ta@mc.pref.osaka.jp

Bacterial components activate innate immune cells, including dendritic cells (DCs), through Toll-like receptors (TLR). This leads to the activation of acquired immune cells, such as CTL, which can directly kill tumor cells. The identification of the TLR family advanced our understanding of DC function and the roles of immunoadjuvants, because most microbial immunoadjuvants work as TLR ligands.[1,2] These findings provide the scientific basis for the development of effective immunoadjuvants.

Previous reports have shown that a cell-wall skeleton fraction of Mycobacterium bovis bacillus Calmette-Guérin (BCG-CWS), which is a ligand for TLR2 and 4, activates DCs to induce antitumor cytotoxic activity *in vitro* and in mouse experimental models *in vivo*.[3,4] BCG-CWS has also been shown to increase the effectiveness of antitumor peptide vaccine therapy.[5] In addition, we have shown that treatment with BCG-CWS after surgery improves the prognosis for patients with non-small-cell lung cancer.[6] Although BCG-CWS is effective as an antitumor immunoadjuvant, the macromolecule is difficult to chemically synthesize and modify.

Clinical trials and basic researches of cancer peptide vaccines in recent years have resulted in suggestions that a new

What's new?

Adjuvants have been used for over 30 years to stimulate the immune response against tumor cells. However, standard immunoadjuvants have not worked as well as might be hoped, and they often cause undesirable local inflammation. In this study, the authors engineered a lipopeptide that functions as a novel toll-like receptor 2 (TLR2) ligand, selectively activating dendritic cells (DCs). This engineered molecule was able to induce more efficient antitumor effects in vivo than standard immunoadjuvants. It also did not cause local inflammation, making it a promising candidate for clinical applications.

efficient immunoadjuvant is needed for cancer vaccine therapy.[7-9] Materials such as alum, mineral oil, Freund's complete/incomplete adjuvant, and mycobacterium components have been used as immunoadjuvants for more than 30 years. New adjuvants must be developed based on recent scientific advancements. Macrophage-activating lipopeptide (MALP)-2 is a lipopeptide of mycoplasmic origin and acts as a TLR2 ligand, similar to BCG-CWS.[10-12] The N-terminal cysteine of the hydrophilic peptide of bacterial origin is modified with two palmitates (Pam2Cys or P2C). The crystal structure analysis of the binding of lipopeptides to TLR2 has already been reported.[13,14] Although lipopeptides have been developed as immunoadjuvants using various methods,[15-17] here, we engineered lipopeptides that function as novel TLR2 ligands with alternative functions by replacing the peptide of bacterial origin with a hydrophilic functional motif.

We previously designed the lipopeptide P2CRGDS *via* this strategy.[18] The RGDS peptide binds to the integrin molecules such as αV/β3 and α5β1, which are expressed on DCs.[19,20] To enhance the antitumor immunoactivity of the lipopeptide by increasing its ability to bind to DCs, P2C was conjugated to the RGDS peptide. P2CRGDS activated DCs and splenocytes more efficiently over short incubation times *in vitro* and showed a greater ability to inhibit tumor growth *in vivo* than MALP-2. However, P2CRGDS induced severe inflammation at the vaccination site that correlated with the antitumor effect, similarly to another artificial lipopeptide, P2CSK4.[21-23] The RGDS peptide of P2CRGDS could bind to many integrin-expressing cells, such as other immune cells and epithelial cells present at the vaccination site. In addition, the KKKK sequence of P2CSK4, which is composed of four positively charged lysines, could have a nonspecific ionic affinity to negative charged species on the plasma membrane of cells. Therefore, these lipopeptides may nonspecifically bind and activate various cells at the vaccination site.

To avoid this local inflammation, we developed a lipopeptide with a CD11c-specific binding sequence that selectively targets DCs. CD11c, which associates with CD18 to form complement receptor 4, is well known as a marker of DCs. Frick *et al.* identified a circular peptide that binds to CD11c/CD18 by panning random peptide phage display libraries over purified CD11c/CD18.[24] They identified a phage expressing the circular peptide C-GRWSGWPADL-C, which shares homology with the D4 domain of intracellular adhesion molecule (ICAM)-1(PEDNGRSFS). Here, we have newly developed DC-targeting lipopeptide, h11c (P2C-ATPEDNGRSFS), to maintain antitumor immunity while avoiding the undesirable immune responses that lead to local inflammation.

Material and Methods

Mice, cells, and reagents

Wild-type and TLR2-/- C57BL/6 mice were purchased from CLEA Japan (Tokyo, Japan). The mice were maintained under specific pathogen-free conditions in the animal facility of the Osaka Medical Center. All animal experiments were performed in accordance with institutional guidelines and approved by the Animal Care and Use Committee of the Osaka Medical Center for Cancer and Cardiovascular Diseases.

Ovalbumin-expressing EL4 thymoma cells (E.G7-OVA cells) were obtained from the American Tissue Culture Collection (ATCC) (Manassas, VA).[25] A subline of B16 melanoma cells, B16D8, was established in our institute.[26] A murine Wilms tumor 1 (WT1)-expressing acute myeloid leukemia cell line (mWT1-C1498) was kindly provided by Dr. H. Sugiyama (Osaka University, Osaka, Japan).[27] RMA-S, a TAP2-deficient subline of RMA (Rauscher leukemia virus-induced lymphoma cell line), was kindly provided by Dr. K. Kärre (Karolinska Institute, Sweden). All cell lines were cultured in RPMI 1640 supplemented with 10% heat-inactivated fetal bovine serum (FBS), 100 U mL^{-1} penicillin, and 100 μg mL^{-1} streptomycin at 37°C in a 5% CO_2 atmosphere. The E.G7-OVA cells were cultured in medium additionally supplemented with 10 mmol L^{-1} HEPES (pH 7.3), 1 mmol L^{-1} sodium pyruvate, 55 μmol L^{-1} 2-mercaptoethanol, and 400 μg mL^{-1} G418, and the mWT1-C1498 cells were cultured in medium additionally supplemented with 55 μmol L^{-1} 2-mercaptoethanol and 500 μg mL^{-1} G418. Cell lysates were prepared by the freeze-thaw method.

Peptides and lipopeptides

Peptides, lipopeptides, and FITC-labeled lipopeptides (purity > 90%) were customized by Bio-Synthesis (TX, USA) *via* Biologica (Aichi, Japan). Peptides and lipopeptides were synthesized as follows: OVA peptide, SIINFEKL; murine WT1 peptide, RMFPNAPYL[28]; h11c lipopeptide, P2C-ATPEDNGRSFS; P2CSK4 lipopeptide, P2C-SKKKK; and MALP2 lipopeptide, P2C-GNNDESNISFKEK. The peptide portions of the lipopeptides were synthesized by Fmoc-based solid-phase chemistry.

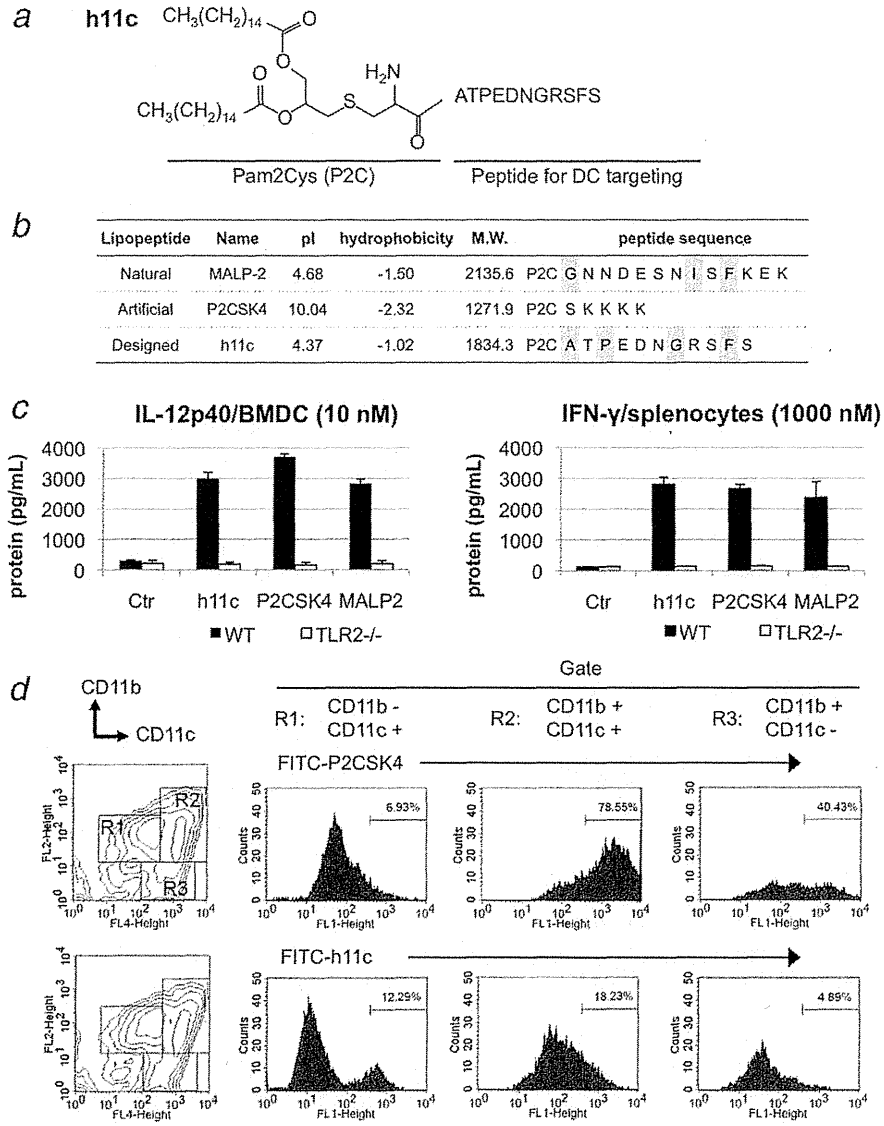

Figure 1. Structure and characteristics of a novel lipopeptide designed to target DCs *via* TLR2. (*a*) The structure of h11c. The lipopeptide h11c (P2C-ATPEDNGRSFS) consists of an N-terminal cysteine modified with two palmitates (Pam2Cys, P2C) and a C-terminal CD11c-binding peptide, ATPEDNGRSFS. (*b*) The structure, molecular weight, isoelectric point (pI), and hydrophobicity of natural (MALP-2) and synthetic (h11c and P2CSK4) lipopeptides used in this study. The pI and hydrophobicity of the peptide portion were calculated using the ProtParam tool (http://br.expasy.org/tools/protparam.html). The gray boxes indicate hydrophobic amino acids. (*c*) IL-12p40 production by BMDCs (left) and IFN-γ production by splenocytes (right) stimulated with each lipopeptide in wild type and TLR2 knockout mice. (*d*) The selectivity of h11c to CD11c+ or CD11b+ cells. Bone marrow cells cultured with GM-CSF were incubated with FITC-lipopeptide for 6 hr at 37°C. Representative images and FACS data from two experiments with similar results are shown.

N-fluorenylmethoxycarbonyl- S-2, 3-bis (palmitoyloxy)-(2-RS)-propyl- (R)-cysteine (Fmoc-Pam2Cys) were coupled with the peptide using standard coupling reagents. Fluorescein isothiocyanate (FITC)-labeled lipopeptides were composed of FITC-aminohexanoic acid linking to an amino group of the N-terminal cysteine of the lipopeptide.

Preparation of mouse BMDCs, splenocytes, and lymph node cells

Bone marrow-derived DCs (BMDCs) were prepared as previously described.[29,30] Inguinal lymph node cells and splenocytes were prepared using Lympholyte-M (Cedarlane, Ontario, Canada). CD11c+ or CD11b+ cells were separated

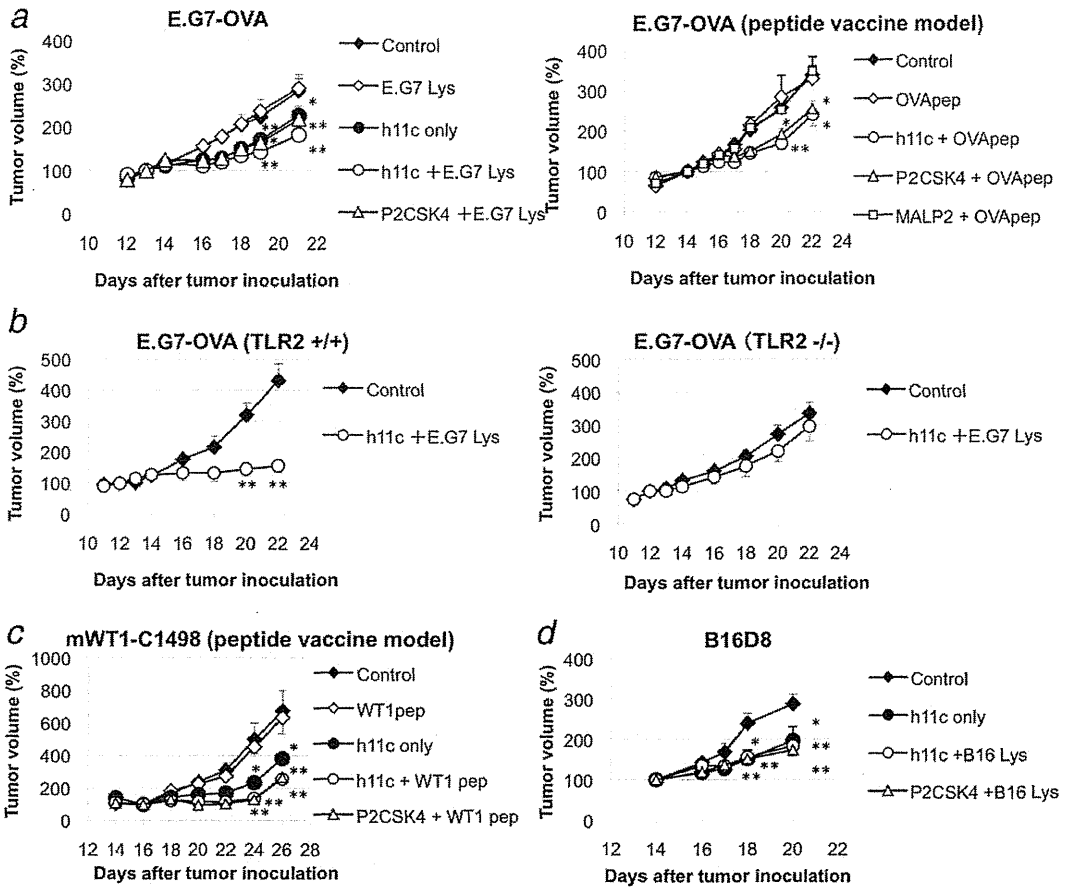

Figure 2. The antitumor effects of lipopeptides in mouse models. (*a*) The antitumor effects of h11c, P2CSK4 and MALP2 were evaluated in mice bearing E.G7-OVA tumors. The lipopeptides were subcutaneously injected around the tumor with tumor cell lysate (left panel) or OVA peptide (right panel) as a tumor antigen on days 13, 16 and 20. (*b*) The antitumor activity of lipopeptide in E.G7-OVA tumors in TLR2 KO mice. (*c*) Significant suppression of tumor growth by h11c in the mWT1-C1498 model. (*d*) In the MHC class I-negative B16D8 melanoma model, h11c induced similar antitumor activity when administered alone or with tumor lysate. Data are representative of more than two independent experiments and are shown as the average + SE $*p < 0.05$, $**p < 0.01$ (*vs.* untreated control group). Each experiment was performed using more than five mice per group.

from total splenocytes with CD11c or CD11b microbeads (MACS system; Miltenyi Biotec, Auburn, CA).

In vitro stimulation assays

For the *in vitro* stimulation assays, BMDCs and splenocytes were stimulated with the synthesized lipopeptide (10 nmol L^{-1} for BMDCs, 1,000 nmol L^{-1} for splenocytes and 100 nmol L^{-1} for cells isolated by MACS) or with 10 μg mL^{-1} BCG-CWS. BMDCs were stimulated for 24 hr for FACS analysis and 48 hr for ELISA analysis, and splenocytes were stimulated for 72 hr for ELISA analysis. For the stimulation assays over short incubation with lipopeptide, after stimulation with TLR2 ligands at 4°C for 60 min, the cells were then washed and recultured for 72 hr. To exclude the possible effects of contamination with lipopolysaccharide, all lipopeptides were pretreated with polymyxin B (Sigma–Aldrich Chemical Company, St. Louis, MO) at 37°C for 60 min.

FACS analysis, ELISA, H&E staining and immunostaining

The following antibodies were used for FACS analysis: FITC-conjugated anti-mouse CD80, phycoerythrin (PE)-conjugated anti-mouse CD11b, and allophycocyanin (APC)-conjugated anti-CD11c (eBioscience, San Diego, CA). For evaluation of secreted proteins, culture supernatants were analyzed with ELISA kits for IFN-γ, IL-12p40, IL-6 and macrophage inflammatory protein (MIP)−2 (R&D Systems, Minneapolis, MN). H&E staining was performed using standard methods. For immunostaining, frozen sections were fixed with cold acetone for 30 min and incubated for 30 min at room temperature with FITC-anti-CD31, FITC-anti-CD11b, PE-anti-Gr-1, PE-anti-CD8α or PE-anti-CD11c antibodies.

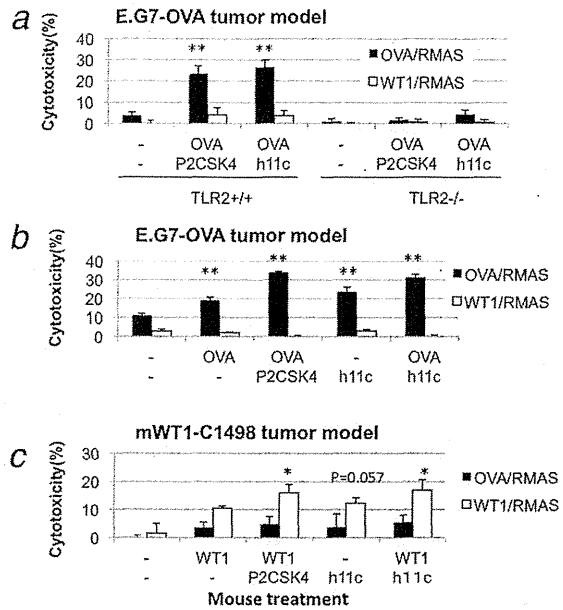

Figure 3. CTL induction by lipopeptides in tumor-bearing mice. (*a* and *b*) Splenocytes were harvested from mice with E.G7-OVA tumors treated with the lipopeptide plus OVA peptide. After *in vitro* culture with OVA peptide and IL-2 for 6 days, the cytotoxic activity against RMA-S cells pulsed with the OVA peptide (black bars) or the WT1 control peptide (white bars) was measured by ^{51}Cr release assay. Tumor-specific CTLs were induced *via* TLR2 activation (*a*) or by stimulation with lipopeptide alone (*b*). (*c*) In the mWT1-C1498 tumor model, WT1 peptide-specific cytotoxic activity was measured. Data are representative of two independent experiments and are shown as the average + SD $*p < 0.05$, $**p < 0.01$. (*vs.* control splenocytes derived from untreated tumor-bearing mice).

In vivo therapy models

For experiments with E.G7-OVA cells, mice were shaved on the back and injected subcutaneously with 200 μL of 1–2 × 10^6 syngeneic E.G7-OVA cells in PBS on day 0. Treatments were administered three times/week on days 14–24. A mixture (50 μL) consisting of 10 nmol of lipopeptide and lysate from 2 × 10^5 E.G7-OVA cells or 10 nmol OVA peptide was injected intradermally around the transplanted tumor. Tumor volume was measured as previously described.[18] For experiments with mWT1–1498 cells, mice were subcutaneously implanted with 3 × 10^5 cells in 100 μL of PBS on the right flank. The mice were treated with mWT1 peptide as in the E.G7-OVA model. In the B16D8 melanoma model, mice were subcutaneously injected on the back with 6 x 10^5 syngeneic B16D8 melanoma cells in 200 μL of PBS on day 0.[31]

Cytotoxicity assay

For analysis of CTL activity, the mice were treated with the same protocol as in the *in vivo* therapy models. The mice were sacrificed 24 hr after the third treatment, and the splenocytes were cultured with 20 U mL^{-1} recombinant murine IL-2 (PeproTech, London, UK) and 5 μg mL^{-1} antigen peptide. Additional IL-2 was added to the culture medium at a concentration of 20 U mL^{-1} 2 and 4 days later. After 6 days of culture, ^{51}Cr release cytotoxicity assays were performed against WT1 peptide-pulsed or OVA peptide-pulsed RMA-S cells. The percentage of specific lysis was calculated as previously described.[18]

Analysis of the biokinetics and selectivity of FITC-conjugated lipopeptides

For an analysis of the biokinetics of the lipopeptides *in vivo*, mice bearing E.G7-OVA tumors were intradermally injected with a 50 μL of a mixture consisting of 10 nmol of FITC-conjugated lipopeptide and the cell lysate of 2 × 10^5 E.G7-OVA cells, adjacent to the transplanted tumor mass. Twenty-four hours after the injection, the mice were sacrificed and tissue samples were prepared from the skin around the administration site, the tumor, the draining lymph node, and the spleen.

For an analysis of the selectivity of the lipopeptides *in vitro*, BMDC were treated with 100 nmol L^{-1} of FITC-conjugated lipopeptides in culture medium for 6 hr at 37°C. BMDCs were washed and then incubated for 30 min at 4°C with PE-conjugated anti-mouse CD11c and APC-conjugated anti-CD11b antibodies (eBioscience) and analyzed by FACS.

Statistical analyses

For measurements of cytokine levels and tumor volumes, the data represent the average ± SD (for cytokines) or the average ± standard error (SE) (for tumor volumes). Statistically significant differences between groups were analyzed by the Student's *t* test in all experiments. A p value of < 0.05 was considered significant.

Results

The structure and characteristics of the DC-targeting lipopeptide, h11c

We designed a DC-targeting lipopeptide, h11c (P2C-ATPEDNGRSFS), composed of a cysteine conjugated with two palmitates (P2C) and a CD11c-targeting peptide (ATPEDNGRSFS) (Fig. 1*a*). The peptide is derived from human ICAM-1 and shares homology with a cyclic peptide with affinity to human CD11c/CD18. We expected that this lipopeptide would selectively activate DCs but not other immune cells. The water solubility and isoelectric point (pI) of the lipopeptide are similar to those of MALP-2, but different from those of the artificial lipopeptide P2CSK4 (Fig. 1*b*).

Firstly, we investigated the ability of these lipopeptides to activate immune cells. The h11c lipopeptide induced IL-12p40 production by BMDCs and IFN-γ production by splenocytes as efficiently as P2CSK4 and MALP2, in a dose-dependent manner (Supporting Information Figs. 1*a* and 1*b*). The induction of these cytokines by h11c was dependent on TLR2 (Fig. 1*c*). Moreover, h11c induced the expression of CD80, a known DC maturation marker, in wild-type but not TLR2-knockout (KO) DCs (Supporting Information Fig. 1*c*).

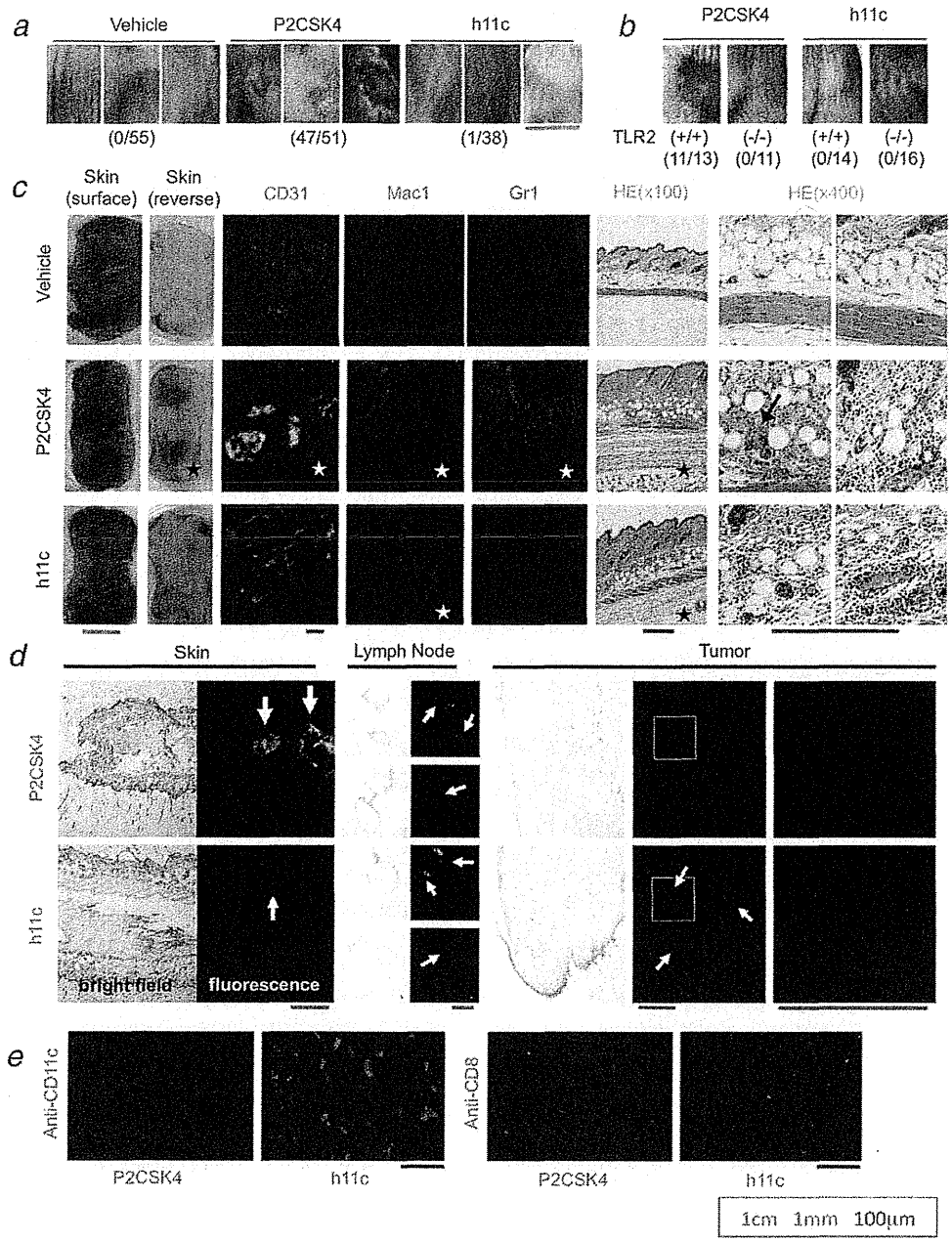

Figure 4. Histopathological analysis of the skin vaccination site and tumor. (*a* and *b*) Skin reactions at the vaccination site of tumor-bearing mice treated as shown in Figure 2. (*c*) Normal mice were injected with 10 nmol lipopeptide and E.G7-OVA lysate. Five days later, the skin at the vaccination site was prepared for frozen or paraffin-embedded sections. Samples were stained with the indicated antibodies or methods. White and black stars indicate differences observed between the treatment groups with respect to inflammation and hyperplasia, CD31 expression (as a marker of angiogenesis), CD11b expression (as a marker of macrophages), and Gr-1 expression (as a marker of neutrophil accumulation). In H&E staining analysis, hemorrhagic lesions (black arrow) were observed in only P2CSK4-vaccinated mice. (*d*) Analysis of biokinetics of FITC-conjugated lipopeptides. The skin, draining lymph nodes and tumors were prepared 24 hr after the injection of FITC-P2CSK4 (upper panels) or FITC-h11c (lower panels). (*e*) CD11c+ cells and CD8+ cells infiltrated into the tumors in mice treated with FITC-h11c more efficiently than in mice treated with FITC-P2CSK4. Red, CD8+ or CD11c+ cells; green, FITC-conjugated lipopeptides. Red line: 1 cm, green line: 1 mm, blue line: 100 μm.

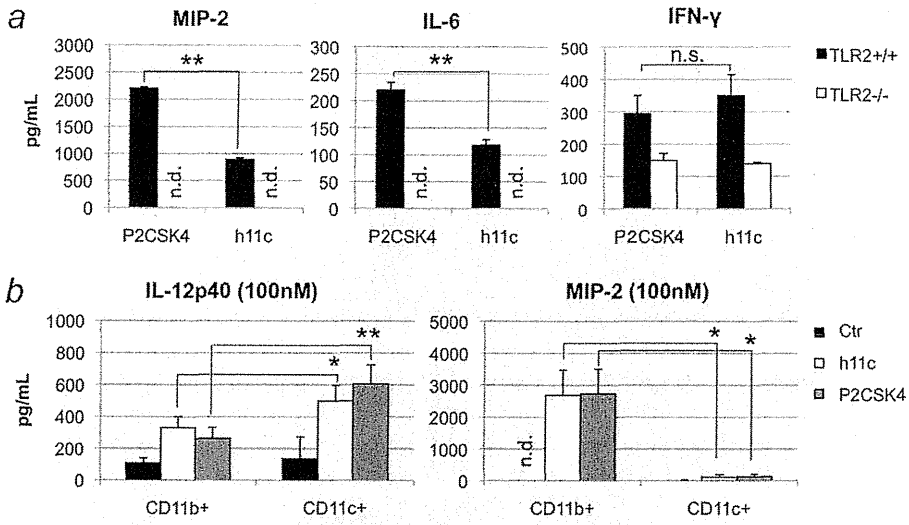

Figure 5. Differences in cytokines and chemokines produced by splenocytes in response to stimulation with h11c and P2CSK4. (*a*) TLR2-dependent production of cytokines and chemokines. MIP-2 (left), IL-6 (middle) and IFN-γ (right) production by splenocytes in stimulation assay over short incubation with lipopeptides. The splenocytes stimulated with h11c produced less MIP-2 and IL-6 than those stimulated with P2CSK4. (*b*) The production of IL-12p40 (left) and MIP-2 (right) by isolated CD11b+ or CD11c+ cells stimulated with lipopeptides. IL-12p40 was produced by both CD11b+ and CD11c+ cells, while MIP-2 was specifically produced by CD11b+ cells. Data are shown as the average + SD $*p < 0.05$, $**p < 0.01$. n.d., not detected; n.s., not significant.

Next, we examined the affinity of FITC-conjugated lipopeptides for various immune cell subpopulations in bone marrow cells cultured with granulocyte-macrophage colony-stimulating factor (GM-CSF) for 5 days (Fig. 1*d*). FITC-h11c selectively bound to CD11c+ cells, while FITC-P2CSK4 mainly bound to CD11b+ cells. These data suggest that h11c selectively activate CD11c+ DCs *in vitro*.

Antitumor activity of h11c in experimental mouse models

To investigate the antitumor immunoadjuvant activity of h11c *in vivo*, mice bearing E.G7-OVA tumors were treated with the lipopeptide plus/minus E.G7-OVA cell lysate (Fig. 2*a*, left) or OVA peptide (Fig. 2*a*, right). Treatment with h11c resulted in significant antitumor effects even without an OVA antigen source. Combination treatment with h11c and tumor lysate increased the antitumor activity compared to that of h11c alone (Fig. 2*a*). The antitumor effect of h11c was dependent on TLR2 (Fig. 2*b*). Moreover, h11c also showed strong antitumor effects in two other models, the mWT1-C1498 tumor model, which is sensitive to vaccination with WT1 peptide (Fig. 2*c*),[27] and the B16 melanoma model, which is susceptible to lysis by natural killer (NK) cells (Fig. 2*d*).[31,32] The addition of tumor lysate did not affect the antitumor activity of h11c in the B16 melanoma model. At a high dose of lipopeptide (10 nmol), P2CSK4 and h11c had equivalent antitumor activity, while MALP-2 treatment had no effect on tumor growth (Fig. 2). However, h11c had a stronger antitumor effect than P2CSK4 at a low dose of lipopeptide (1 or 3 nmol), indicating that h11c is more efficient than P2CSK4 at inducing antitumor immune responses (Supporting Information Fig. 2).

Efficient CTL induction by h11c

To examine whether mice treated with the lipopeptide and antigen peptide acquire antigen-specific cytotoxic activity in the E.G7-OVA and mWT1-C1498 tumor models, a ^{51}Cr release assay was performed using peptide-pulsed RMA-S cells as targets. In E.G7-OVA tumor-bearing mice treated with lipopeptide and OVA peptide, OVA-specific CTLs were efficiently induced by h11c and P2CSK4 to the same extent, in a TLR2-dependent manner (Fig. 3*a*). Interestingly, OVA-specific CTLs were induced in E.G7-OVA mice treated with h11c alone (Fig. 3*b*). Because tumor-bearing mice had already been exposed to the tumor and its antigens *in vivo*, it was possible to induce tumor-specific CTLs even without antigen peptide in the vaccine. Furthermore, in another tumor model in which mWT1-C1498 tumor-bearing mice were treated with h11c or P2CSK4, WT1-specific CTLs were also induced (Fig. 3*c*). These results suggest that both h11c and P2CSK4 have the ability to induce antigen-specific CTL.

Skin reactions to lipopeptide at the vaccination site

Although there were no significant differences in the antitumor effects of the h11c and P2CSK4 lipopeptides at doses of 10 nmol/mouse, severe inflammatory symptoms such as redness, ulcers, and necrosis were observed in the skin near the injection

site of 47 out of 51 mice treated with P2CSK4 (Fig. 4*a*). This effect was dependent on TLR2 (Fig. 4*b*). However, these inflammatory effects were not observed at the h11c injection sites.

Next, non-tumor-bearing mice were injected intracutaneously with the lipopeptides and the skin around the injection site was analyzed immunohistochemically (Fig. 4*c*). In the P2CSK4 injection sites, severe inflammation was observed, with infiltration of inflammatory cells, notable epidermal hyperplasia, and hemorrhaging evident upon H&E staining. In addition, increased vascularization and infiltration of granulocytes was detected using fluorescent immunostaining with anti-CD31 and Gr-1 antibodies, respectively. Infiltration of CD11b+ macrophages and mild increases in vascularization were also detected around the injection sites in mice administered h11c, but infiltration of Gr-1+ granulocytes was not observed. Because P2CSK4 induced this local inflammatory reaction at the administration site, even at 1/10 of the dose of h11c (1 *vs.* 10 nmol), the pro-inflammatory effect of P2CSK4 is at least 10-fold greater than that of h11c (Supporting Information Fig. 3).

Biokinetics of FITC-conjugated h11c

To elucidate the mechanism by which P2CSK4 but not h11c induced severe inflammation around the vaccination site, the biokinetics of FITC-conjugated lipopeptides were examined in mice bearing E.G7-OVA tumors 24 hr after peritumoral administration (Fig. 4*d*). Most P2CSK4 had accumulated in the skin around the administration site, and small amounts of P2CSK4 were detected in the draining lymph node, but very little P2CSK4 was detected in the tumor mass. Meanwhile, h11c was rapidly cleared from the administration site and was detected in the draining lymph node and the tumor (Fig. 4*d*). Furthermore, CD11c+ cells and CD8+ cytotoxic T cells infiltrated the tumors of mice treated with h11c more effectively than those treated with P2CSK4 (Fig. 4*e*).

Selectivity of lipopeptide for DCs or macrophages affects the splenic cytokine profiles

To examine the mechanism through which Gr-1+ granulocytes selectively infiltrated the P2CSK4 injection sites, the cytokine profiles of splenocytes in the stimulation assays over short incubation with P2CSK4 or h11c were examined. P2CSK4 induced significantly more MIP-2 and IL-6 than h11c, but the expression of IFN-γ was not different between P2CSK4 and h11c (Fig. 5*a*). Furthermore, h11c and P2CSK4 acted on isolated CD11b+ cells and CD11c+ cells to induce the production of IL-12p40, but induced the production of MIP-2 only in CD11b+ cells (Fig. 5*b*). MIP-2 is a selective chemotactic factor for granulocytes and is secreted by macrophages. These results suggest that h11c selectively stimulates CD11c+ DCs in the spleen and avoids inducing the production of MIP-2 from CD11b+ macrophages.

Discussion

We developed a novel candidate for an antitumor immunoadjuvant, h11c, through our adjuvant engineering project. An ideal lipopeptide immunoadjuvant should have the ability to activate DCs at low doses and should avoid the activation of the other immune cells. Indeed, although P2CSK4 induced efficient antitumor effects, it also induced severe local inflammation at the vaccination site. In contrast, h11c retained the antitumor activity similarly to P2CSK4 while avoiding the induction of local inflammation (Figs. 2 and 4*a*). Moreover, h11c showed stronger antitumor activity than P2CSK4 at low doses (Supporting Information Fig. 2). Although inflammation at the vaccination site has been regarded as an index of immune activation, this is a side effect to be avoided for patients. On the other hand, h11c induced strong antitumor effects when mixed with various types of antigens such as peptides or protein in saline solution (Fig. 2). Moreover, because antitumor effects and tumor-specific CTLs were induced by h11c alone, it may be possible to apply h11c widely to tumor-bearing patients even when the immunodominant tumor antigens have not been identified.

In this study, we report two mechanisms by which h11c fails to induce the local inflammation that is often observed at the site of administration of other lipopeptides. First, h11c induced less production of MIP-2 from stimulated mouse splenocytes than P2CSK4 (Fig. 5*a*). MIP-2 is a chemotactic factor for neutrophils produced by CD11b+ macrophage but not CD11c+ DCs (Fig. 5*b*),[33,34] and numerous Gr-1+ neutrophil-like cells were detected invading the skin at the site of P2CSK4 administration (Fig. 4*c*). These results suggest that h11c may avoid inducing local inflammation by selectively activating DCs and not macrophages. Indeed, h11c seems to have the ideal properties of an adjuvant, in that it selectively binds to CD11c+ cells (Fig. 1*d*) and induces significant antitumor activity (Fig. 2) without inducing MIP-2 production and neutrophils accumulation leading to local inflammation at the vaccination site (Figs. 4*a*, 4*c*, and 5*a*). In *in vitro* experiments, IL-6 and MIP-2 production by splenocytes in response to P2CSK4 was higher than the response induced by h11c. However, different responses to P2CSK4 and h11c were only observed in cultures of total splenocytes, and both lipopeptides induced similar amounts of cytokines when BMDC were stimulated. It might be that the cultivation of large amounts of purified cells with a high concentration of lipopeptide induced a maximal response.

The second mechanism accounting for the superior toxicity profile of h11c lies in the observation that h11c was quickly cleared from the injection site and transported to the lymph node and tumor site. In contrast, most P2CSK4 was retained at the injection site for more than a day (Fig. 4*d*), where it could continuously activate TLR2 on macrophages and other cells and induce local inflammation. P2CSK4 may nonspecifically bind to the negatively charged cell membrane by its positively charged poly-lysines and thereby be retained at the vaccination site. Although both P2CSK4 and h11c were similarly transported from the vaccination site to the tumor-draining lymph node (Fig. 4*d*), h11c was also transported into the tumor by blood circulation or diffusion. It is also possible that h11c was

transported into the tumor by DCs, because many DCs were detected in the tumors of h11c-treated mice and co-localized with h11c. Based on the localization of the lipopeptides, it appears that P2CSK4 activated immune cells within the skin, causing local inflammation, while h11c induced immune activation within the tumor. In a recent report, it was suggested that the accumulation of antigen-specific CTL with local inflammation at the vaccination site (rather than within the tumor itself) was associated with a decreased antitumor effect.[35] Although proper inflammation promotes antitumor immune responses, our results also suggested that the skin inflammation is not necessary for antitumor effects of immunoadjuvants. Our synthetic lipopeptide could serve as a next-generation standard adjuvant to control immune activation at the vaccination site.

All responses to lipopeptides, including activation of BMDCs and splenocytes *in vitro*, and CTL induction and antitumor activity *in vivo*, depend on TLR2. Although the most remarkable difference in the immune responses between h11c and P2CSK4 was the induction of severe inflammation and necrosis at the vaccination site, this response was also dependent on TLR2. Microarray analysis of BMDCs and splenocytes stimulated with h11c or P2CSK4 failed to identify differences in TLR2 signaling, but other signals were differentially induced by each lipopeptide. Therefore, we assume existence of a second signal or receptor dependent on the peptide sequence.[36–40] The adverse effects of the lipopeptide may therefore be due not only to simple skin retention of the lipopeptide and the selectivity of DCs or macrophages for the lipopeptide, but also to differences in signaling. A more detailed analysis of this point is required.

Although h11c was designed based on the human ICAM-1 sequence,[41] m11c-T (P2C-AREEDDGRTLS), which was designed based on the mouse testicular cell adhesion molecule, TCAM-1,[42] was also evaluated. Mouse TCAM-1 shares homology with mouse ICAM-1. These two lipopeptides have similar characteristics and induce strong antitumor activity without severe inflammation at the vaccination site. Two additional lipopeptides, m11c-I (P2C-ASSEDHKRSFF), which was based on the mouse ICAM-1 sequence,[43] and d11c (P2C-ASAADNRRSFS), which was based on the canine ICAM-1 sequence,[44] were also generated. Unlike h11c, these lipopeptides induced local inflammation at the vaccination site. Interestingly, in an *in vivo* mouse experimental model, the lipopeptide based on the human ICAM-1 sequence or the mouse TCAM-1 sequence showed more ideal responses with respect to side effects than the lipopeptide based on the mouse ICAM-1 sequence. These results suggest that not only the binding motif but also other characteristics of the lipopeptide, such as its pI or hydrophobicity, may influence its activity.

MALP-2, a natural lipopeptide derived from mycoplasma, did not induce a strong antitumor effect in this study. However, human clinical trials of MALP-2 with favorable results have already been reported.[45] Because h11c shows greater antitumor activity than MALP-2 in mouse models, we expect that h11c will also show favorable antitumor immune responses in human patients. We intend to accelerate the use of h11c in human clinical trials by evaluating the validity and safety of h11c in a veterinary setting.[46]

Acknowledgements

The authors are grateful to Drs. M. Matsumoto, T. Seya (Hokkaido University), K. Kato, and M. Hori (Osaka Medical Center for Cancer and Cardiovascular diseases) for their support of this work and Dr. H. Sugiyama (Osaka University) for providing mWT1-C1498. Thanks are also due to T. Yasuda, N. Kanto and H. Murakami for their assistance (Osaka Medical Center for Cancer and Cardiovascular diseases).

References

1. Kaisho T, Akira S. Toll-like receptors as adjuvant receptors. *Biochim Biophys Acta* 2002;1589:1–13.
2. Hemmi H, Takeuchi O, Kawai T, et al. A Toll-like receptor recognizes bacterial DNA. *Nature* 2000;408:740–5.
3. Tsuji S, Matsumoto M, Takeuchi O, et al. Maturation of human dendritic cells by cell wall skeleton of Mycobacterium bovis bacillus Calmette-Guerin: involvement of toll-like receptors. *Infect Immun* 2000;68:6883–90.
4. Akazawa T, Masuda H, Saeki Y, et al. Adjuvant-mediated tumor regression and tumor-specific cytotoxic response are impaired in MyD88-deficient mice. *Cancer Res* 2004;64:757–64.
5. Nakajima H, Kawasaki K, Oka Y, et al. WT1 peptide vaccination combined with BCG-CWS is more efficient for tumor eradication than WT1 peptide vaccination alone. *Cancer Immunol Immunother* 2004;53:617–24.
6. Kodama K, Higashiyama M, Takami K, et al. Innate immune therapy with a Bacillus Calmette-Guerin cell wall skeleton after radical surgery for non-small cell lung cancer: a case-control study. *Surg Today* 2009;39:194–200.
7. Rosenberg SA, Yang JC, Restifo NP. Cancer immunotherapy: moving beyond current vaccines. *Nat Med* 2004;10:909–15.
8. Celis E. Toll-like receptor ligands energize peptide vaccines through multiple paths. *Cancer Res* 2007;67:7945–7.
9. Muraoka D, Kato T, Wang L, et al. Peptide vaccine induces enhanced tumor growth associated with apoptosis induction in CD8+ T cells. *J Immunol* 2010;185:3768–76.
10. Muhlradt PF, Kiess M, Meyer H, et al. Isolation, structure elucidation, and synthesis of a macrophage stimulatory lipopeptide from Mycoplasma fermentans acting at picomolar concentration. *J Exp Med* 1997;185:1951–8.
11. Matsumoto M, Nishiguchi M, Kikkawa S, et al. Structural and functional properties of complement-activating protein M161Ag, a Mycoplasma fermentans gene product that induces cytokine production by human monocytes. *J Biol Chem* 1998;273:12407–14.
12. Takeuchi O, Hoshino K, Kawai T, et al. Differential roles of TLR2 and TLR4 in recognition of gram-negative and gram-positive bacterial cell wall components. *Immunity* 1999;11:443–51.
13. Kang JY, Nan X, Jin MS, et al. Recognition of lipopeptide patterns by Toll-like receptor 2-Toll-like receptor 6 heterodimer. *Immunity* 2009;31:873–84.
14. Jin MS, Kim SE, Heo JY, et al. Crystal structure of the TLR1-TLR2 heterodimer induced by binding of a tri-acylated lipopeptide. *Cell* 2007;130:1071–82.
15. Hida T, Hayashi K, Yukishige K, et al. Synthesis and biological activities of TAN-1511 analogues. *J Antibiot (Tokyo)* 1995;48:589–603.
16. Reutter F, Jung G, Baier W, et al. Immunostimulants and Toll-like receptor ligands obtained by screening combinatorial lipopeptide collections. *J Pept Res* 2005;65:375–83.
17. Jackson DC, Lau YF, Le T, et al. A totally synthetic vaccine of generic structure that targets Toll-like receptor 2 on dendritic cells and promotes antibody or cytotoxic T cell responses. *Proc Natl Acad Sci USA* 2004;101:15440–5.
18. Akazawa T, Inoue N, Shime H, et al. Adjuvant engineering for cancer immunotherapy: development of a synthetic TLR2 ligand with increased cell adhesion. *Cancer Sci* 2010;101:1596–603.

19. Okada N, Masunaga Y, Okada Y, et al. Gene transduction efficiency and maturation status in mouse bone marrow-derived dendritic cells infected with conventional or RGD fiber-mutant adenovirus vectors. *Cancer Gene Ther* 2003;10: 421–31.
20. Harui A, Roth MD, Vira D, et al. Adenoviral-encoded antigens are presented efficiently by a subset of dendritic cells expressing high levels of alpha(v)beta3 integrins. *J Leukoc Biol* 2006;79: 1271–8.
21. Muhlradt PF, Kiess M, Meyer H, et al. Structure and specific activity of macrophage-stimulating lipopeptides from *Mycoplasma hyorhinis*. *Infect Immun* 1998;66:4804–10.
22. Omueti KO, Beyer JM, Johnson CM, et al. Domain exchange between human toll-like receptors 1 and 6 reveals a region required for lipopeptide discrimination. *J Biol Chem* 2005;280: 36616–25.
23. Sawahata R, Shime H, Yamazaki S, et al. Failure of mycoplasma lipoprotein MALP-2 to induce NK cell activation through dendritic cell TLR2. *Microbes Infect* 2011;13:350–8.
24. Frick C, Odermatt A, Zen K, et al. Interaction of ICAM-1 with beta 2-integrin CD11c/CD18: characterization of a peptide ligand that mimics a putative binding site on domain D4 of ICAM-1. *Eur J Immunol* 2005;35:3610–21.
25. Helmich BK, Dutton RW. The role of adoptively transferred CD8 T cells and host cells in the control of the growth of the EG7 thymoma: factors that determine the relative effectiveness and homing properties of Tc1 and Tc2 effectors. *J Immunol* 2001;166:6500–8.
26. Tanaka H, Mori Y, Ishii H, et al. Enhancement of metastatic capacity of fibroblast-tumor cell interaction in mice. *Cancer Res* 1988;48:1456–9.
27. Nakajima H, Oka Y, Tsuboi A, et al. Enhanced tumor immunity of WT1 peptide vaccination by interferon-beta administration. *Vaccine* 2012;30: 722–9.
28. Oka Y, Udaka K, Tsuboi A, et al. Cancer immunotherapy targeting Wilms' tumor gene WT1 product. *J Immunol* 2000;164:1873–80.
29. Inaba K, Pack M, Inaba M, et al. High levels of a major histocompatibility complex II-self peptide complex on dendritic cells from the T cell areas of lymph nodes. *J Exp Med* 1997;186:665–72.
30. Akazawa T, Shingai M, Sasai M, et al. Tumor immunotherapy using bone marrow-derived dendritic cells overexpressing Toll-like receptor adaptors. *FEBS Lett* 2007;581:3334–40.
31. Akazawa T, Ebihara T, Okuno M, et al. Antitumor NK activation induced by the Toll-like receptor 3-TICAM-1 (TRIF) pathway in myeloid dendritic cells. *Proc Natl Acad Sci USA* 2007;104: 252–7.
32. Ohashi T, Akazawa T, Aoki M, et al. Dichloroacetate improves immune dysfunction caused by tumor-secreted lactic acid and increases antitumor immunoreactivity. *Int J Cancer* 2013;133: 1107–18.
33. Luhrmann A, Tschernig T, Pabst R, et al. Improved intranasal immunization with live-attenuated measles virus after co-inoculation of the lipopeptide MALP-2. *Vaccine* 2005;23:4721–6.
34. Nance SC, Yi AK, Re FC, et al. MyD88 is necessary for neutrophil recruitment in hypersensitivity pneumonitis. *J Leukoc Biol* 2008;83:1207–17.
35. Hailemichael Y, Dai Z, Jaffarzad N, et al. Persistent antigen at vaccination sites induces tumor-specific CD8+ T cell sequestration, dysfunction and deletion. *Nat Med* 2013;19:465–72.
36. Erdman LK, Cosio G, Helmers AJ, et al. CD36 and TLR interactions in inflammation and phagocytosis: implications for malaria. *J Immunol* 2009;183:6452–9.
37. Shamsul HM, Hasebe A, Iyori M, et al. The Toll-like receptor 2 (TLR2) ligand FSL-1 is internalized via the clathrin dependent endocytic pathway triggered by CD14 and CD36 but not by TLR2. *Immunology* 2010;130:262–72.
38. Azuma M, Sawahata R, Akao Y, et al. The peptide sequence of diacyl lipopeptides determines dendritic cell TLR2-mediated NK activation. *PLoS One* 2010;5:e12550.
39. Seya T, Matsumoto M, Tsuji S, et al. Structural–functional relationship of pathogen-associated molecular patterns: lessons from BCG cell wall skeleton and mycoplasma lipoprotein M161Ag. *Microbes Infect* 2002;4:955–61.
40. Buwitt-Beckmann U, Heine H, Wiesmuller KH, et al. Toll-like receptor 6-independent signaling by diacylated lipopeptides. *Eur J Immunol* 2005; 35:282–9.
41. Degitz K, Li LJ, Caughman SW. Cloning and characterization of the 5'-transcriptional regulatory region of the human intercellular adhesion molecule 1 gene. *J Biol Chem* 1991;266:14024–30.
42. Ono M, Nomoto K, Nakazato S. Gene structure of rat testicular cell adhesion molecule 1 (TCAM-1), and its physical linkage to genes coding for the growth hormone and BAF60b, a component of SWI/SNF complexes. *Gene* 1999;226:95–102.
43. Siu G, Hedrick SM, Brian AA. Isolation of the murine intercellular adhesion molecule 1 (ICAM-1) gene. ICAM-1 enhances antigen-specific T cell activation. *J Immunol* 1989;143:3813–20.
44. Manning AM, Lu HF, Kukielka GL, et al. Cloning and comparative sequence analysis of the gene encoding canine intercellular adhesion molecule-1 (ICAM-1). *Gene* 1995;156:291–5.
45. Schmidt J, Welsch T, Jager D, et al. Intratumoural injection of the toll-like receptor-2/6 agonist 'macrophage-activating lipopeptide-2' in patients with pancreatic carcinoma: a phase I/II trial. *Br J Cancer* 2007;97:598–604.
46. Mito K, Sugiura K, Ueda K, et al. IFN gamma markedly cooperates with intratumoral dendritic cell vaccine in dog tumor models. *Cancer Res* 2010;70:7093–101.

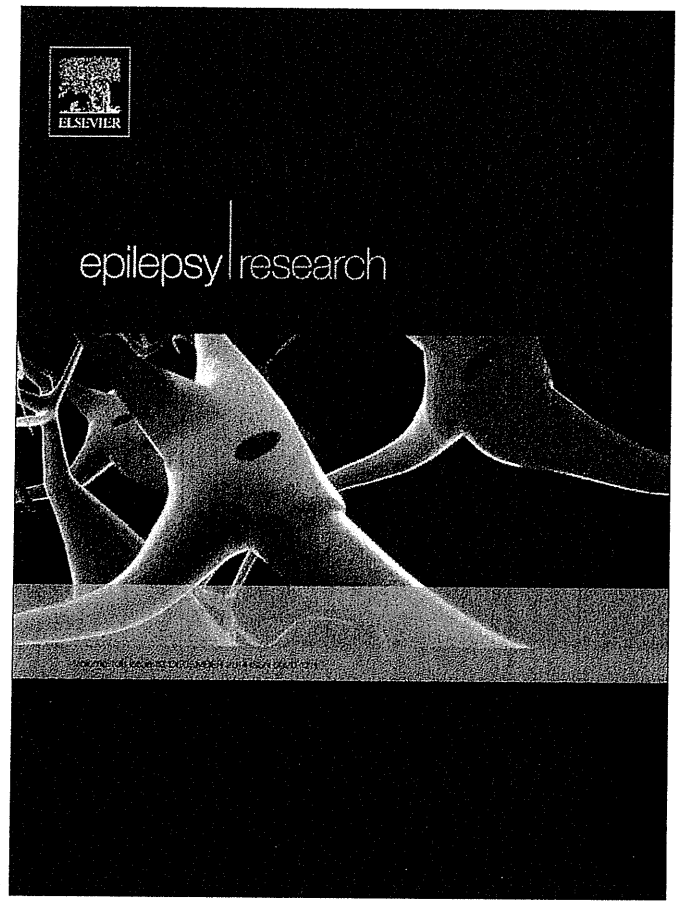

Epilepsy Research (2014) 108, 1845–1852

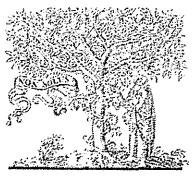

journal homepage: www.elsevier.com/locate/epilepsyres

Developmental outcome after surgery in focal cortical dysplasia patients with early-onset epilepsy

Nobusuke Kimura, Yukitoshi Takahashi*, Hideo Shigematsu, Katsumi Imai, Hiroko Ikeda, Hideyuki Ootani, Rumiko Takayama, Yukiko Mogami, Noriko Kimura, Koichi Baba, Kazumi Matsuda, Takayasu Tottori, Naotaka Usui, Yushi Inoue

National Epilepsy Center, Shizuoka Institute of Epilepsy and Neurological Disorder, NHO, 886 Urushiyama, Aoi-Ku, Shizuoka, Shizuoka, Japan

Received 29 December 2013; received in revised form 11 September 2014; accepted 13 September 2014
Available online 22 September 2014

KEYWORDS
Pediatric epilepsy surgery;
Focal cortical dysplasia;
Development;
Cognition;
Early-onset epilepsy

Summary The purpose of this study was to investigate the developmental outcome after surgery for early-onset epilepsy in patients with focal cortical dysplasia (FCD). Among 108 patients with histopathologically confirmed FCD operated between 1985 and 2008, we selected 17 patients with epilepsy onset up to 3 years of age.

Development was evaluated by the developmental quotient or intelligence quotient (DQ-IQ) and mental age was measured by the Mother-Child Counseling baby test or the Tanaka-Binet scale of intelligence. Postsurgical development outcome was evaluated by the changes in DQ-IQ and mental age as well as rate of increase in mental age (RIMA) after surgery. RIMA was calculated as the increase in mental age per chronological year (months/year; normal average rate: 12 months/year).

Age at epilepsy onset of 17 patients ranged from 15 days to 36 months (mean ± SD, 11.0 ± 10.0 months). Age at surgery ranged from 18 to 145 months (75.1 ± 32.4 months). Evaluation just before surgery showed that 13 of 17 (76.4%) patients had DQ-IQ below 70. Ten patients (58.8%) were seizure-free throughout the postsurgical follow-up period. After surgery, DQ-IQ was maintained within 10 points of the presurgical level in 13 patients (76.4%), and increased by more than 10 points in one patient (5.9%). After surgery, RIMA in patients with Engel's class I (7.5 ± 3.8) was higher than patients with Engel's class II–IV (2.6 ± 3.4) (unpaired t-test with Welch's correction, $t = 2.99$, df = 15, $p = 0.0092$). RIMA was particularly low in two patients with spasm. In four patients with presurgical DQ-IQ < 70, seizure-free after surgery and without spasm, DQ-IQ did not increase but RIMA improved from 3.6 ± 2.8 before surgery to 6.9 ± 2.5 months/year after

* Corresponding author. Tel.: +81 54 245 5446; fax: +81 54 247 9781.
E-mail address: takahashi-ped@umin.ac.jp (Y. Takahashi).

http://dx.doi.org/10.1016/j.eplepsyres.2014.09.010

surgery. RIMA became better from 2 years after surgery. In four patients with presurgical DQ-IQ ≥ 70 and no spasm, two showed the same or higher RIMA than normal average after surgery.
In 58.8% of FCD patients with early onset epilepsy, epilepsy surgery effectively controlled seizures, and in 82.3% of patients, epilepsy surgery preserved or improved development. Residual seizures after surgery and lower DQ-IQ before surgery might be potential risk factors for poor development after surgery. In patients of Engel's class I with lower presurgical DQ-IQ, catch-up increase in mental age was observed after two years following surgery.

Introduction

Focal cortical dysplasia (FCD) was first described in 1971 as 'neuropathology with epilepsy' (Taylor et al., 1971). It is characterized by disorganization of the cerebral cortex, including cortical architectural abnormalities, immature cells, giant neurons, dysmorphic neurons, and balloon cells (Palmini et al., 2004). The embryologic and epileptogenic mechanisms of FCD are not well known (Sisodiya et al., 2009). FCD has been reported to be the etiology in 20–25% of patients with intractable focal epilepsy (Kuzniecky et al., 1993; Tassi et al., 2002; Fauser et al., 2006), and epileptic seizures are poorly controlled by antiepileptic drugs. Epilepsy surgery resulted in complete seizure control in 40–65% of the patients (Tassi et al., 2002; Krsek et al., 2009; Widdess-Walsh et al., 2005).

Regarding the outcome of developmental quotient or intelligence quotient (DQ-IQ) after epilepsy surgery, several studies reported increases in DQ-IQ in patients with early-onset epilepsy who underwent epilepsies surgery in infancy (Wyllie, 1996; Lortie et al., 2002; Loddenkemper et al., 2007). However some studies reported that the majority of patients do not show any significant improvement of DQ-IQ after epilepsy surgery if seizure occurred more than several years (Jonas et al., 2005; Freitag and Tuxhorn, 2005; Argenzio et al., 2011). In this study, we evaluated the developmental outcome after epilepsy surgery in FCD patients with early-onset epilepsy, not only by the evolution of conventional DQ-IQ but also by the evolution of mental age as a trial.

Patients and methods

Patients

We retrospectively evaluated the medical records of 813 patients who underwent epilepsy surgery at the National Epilepsy Center between 1985 and 2008, and found 108 patients with a diagnosis of FCD confirmed by histopathology (Fig. 1). To investigate the post-surgical developmental outcome in pediatric FCD patients with childhood onset epilepsy, we adopted the following exclusion criteria: (1) presence of comorbidity affecting development (one patient with hydrocephalus after surgery, one with Chiari malformation, and one with a history of head trauma); (2) lack of developmental evaluation at two years after surgery (15 patients); (3) more than one surgery (three patients); and (4) age at epilepsy onset ≧15 years (ten patients). Consequently, 77 pediatric patients were identified. To evaluate the developmental outcome in patients with very young onset, we further selected patients who had earlier epilepsy onset using the following inclusion criteria (1) onset of epilepsy ≦3 years of age; (2) age of surgery ≦13 years; (3) evaluation of development by specific psychological tests for children before and after surgery. Eventually 17 patients were studied (Fig. 1).

Classification of subgroups

To analyze the effects of multiple factors affecting developmental outcome after surgery, we classified patients into four subgroups by potential determinants of developmental outcome; namely, seizure outcome, presurgical developmental levels, and presence of spasms (Fig. 2). First, the 17 patients were classified by postsurgical seizure outcome. Seven patients with Engel's class II–IV were classified as group 4 (Patients 11-17). Among ten patients with Engel's class I, four patients with presurgical DQ-IQ ≧ 70 were classified as group 3 (Patients 7-10), and the remaining six patients with presurgical DQ-IQ < 70 were further divided into a group with spasm (group 2; Patients 5 and 6) and a group without spasm (group 1; Patients 1-4).

Pre-surgical evaluation

All patients had poor seizure control despite using more than three antiepileptic drugs. All underwent pre-surgical evaluations including surface electroencephalography (EEG)-video monitoring, brain magnetic resonance imaging, computed tomography, and single-photon emission computed tomography. Seizures were classified as 'daily' if they occurred everyday for at least three months prior to surgery.

Seizure outcome and histopathology after surgery

Seizure outcome was classified using Engel's classification (Engel et al., 1993). Histopathology was classified according to Palmini's classification (Palmini et al., 2004).

Psychological evaluation

Cognitive function was assessed by neuropsychologists. The psychological tests were selected according to the developmental level and chronological age. The

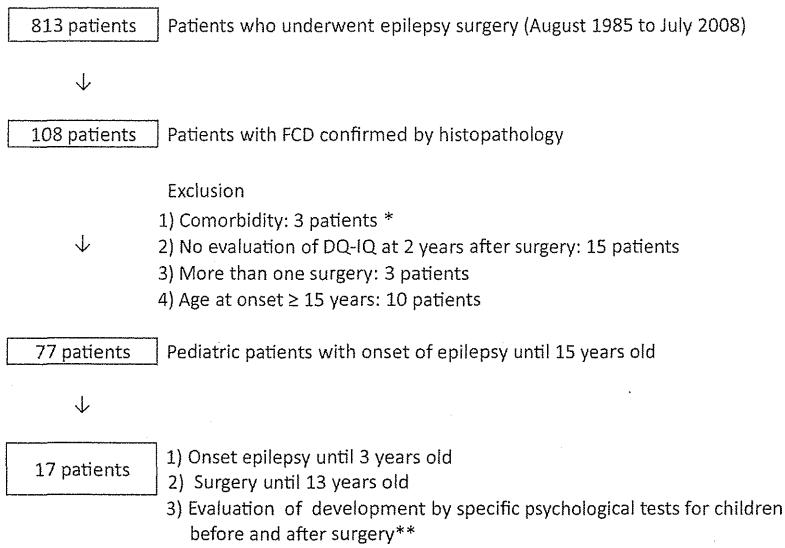

Fig. 1 Selection criteria of patients. FCD, focal cortical dysplasia. * Hydrocephalus after surgery, Chiari malformation, and a history of head trauma in one patient each. ** Tanaka scale or Mother-Child Counseling test.

Mother-Child Counseling baby test (MCC test; Koga, 1967) and the Tanaka-Binet scale of intelligence (Tanaka scale; Tanaka, 1987) were used to assess DQ-IQ and mental age. Postsurgical development was evaluated usually at three month, 1 year and 2 years after surgery in our center. All the psychological tests were performed at intervals longer than 6 months. The same tests were used in pre- and post-surgical evaluations, except for two patients (Patients 1 and 2). For additional evaluation of postsurgical development, we evaluated the rate of increase in mental age (RIMA) in addition to DQ-IQ and mental age. RIMA (months/year) was calculated as follows: mental age at the current evaluation − mental age at the last evaluation (months)/chronological interval between two evaluations (year). Thus normal average of RIMA is 12 months/year.

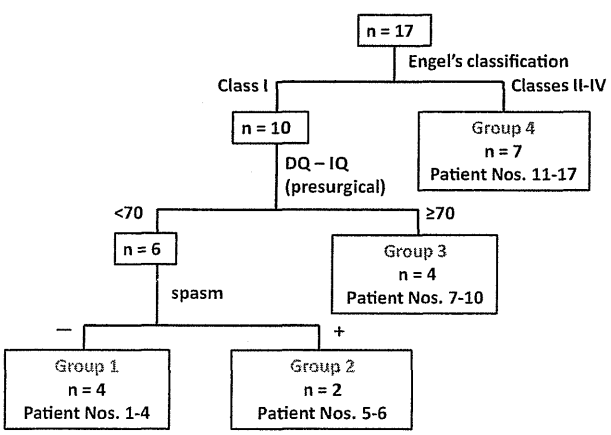

Fig. 2 Grouping of patients. Groups 1–3 were Engel's class I, and group 4 ($n=7$; Patients 11–17) was Engel's class II–IV. Groups 1–2 had presurgical developmental quotient or intelligence quotient (DQ-IQ) < 70. Group 2 ($n=2$; Patients 5 and 6) had presurgical DQ-IQ < 70 and spasm. Group 3 ($n=4$; patients 7–10) had presurgical DQ-IQ ≧ 70 and no spasm.

Statistics

Unpaired t-test with Welch's correction was used to compare RIMA between Engel's class I and class II–IV groups. A P value less than 0.05 was regarded as statistically significant. Group data are presented as mean ± standard deviation unless otherwise stated.

Results

The presurgical clinical profile and surgical outcome of the 17 patients (9 boys and 8 girls) are shown in Table 1. The median age at epilepsy onset was 8.0 months. At the time of presurgical evaluation, all patients had daily seizures, and all but one had complex partial seizures (CPS). Interictal epileptic discharges varied from localized to widespread. On presurgical MRI, FCD was localized in one lobe or distributed in multiple lobes. FCD was proven histopathologically in all patients.

During a mean postsurgical follow-up period of 3.2 years, ten patients were seizure-free (Engel's class I) and seven were not (Engel's classes II–IV).

Table 2 shows the presurgical and postsurgical developmental evaluations. At presurgical evaluation, 14 patients had impaired DQ-IQ (<70) and four had normal DQ-IQ (≧70). The difference in DQ-IQ between the presurgical and the last postsurgical evaluations was less than 10 points in 13 of 17 patients, but one patient showed an increase of 10 points. Three patients showed decreases of more than 10 points.

Comparing the mental age at the last postsurgical evaluation to that at presurgical evaluation, 16 patients showed increases, one patient (Patient 12) showed decrease (Table 2). The patient with decline in mental age belonged to group 4 (no seizure control). Among 16 patients showing